NASA

Technical Memorandum 83964

PRELIMINARY SUBMILLIMETER SPECTROSCOPIC MEASUREMENTS USING A SUBMILLIMETER HETERODYNE RADIOMETER

H. G. Safren, W. R. Stabnow, J. L. Bufton, C. J. Peruso, C. E. Rossey, and H. E. Walker

SEPTEMBER 1982

National Aeronautics and Space Administration

Goddard Space Flight Center
Greenbelt, Maryland 20771

TM 83964

PRELIMINARY SUBMILLIMETER SPECTROSCOPIC MEASUREMENTS USING A SUBMILLIMETER HETERODYNE RADIOMETER

Harvey G. Safren
William R. Stabnow
Jack L. Bufton
Charles J. Peruso
Calvin E. Rossey
Harold E. Walker

September 1982

NASA/Goddard Space Flight Center
Greenbelt, MD 20771

PRELIMINARY SUBMILLIMETER SPECTROSCOPIC MEASUREMENTS

USING A SUBMILLIMETER HETERODYNE RADIOMETER

ABSTRACT

A submillimeter heterodyne radiometer has been under development at the Goddard Space Flight Center for several years. The radiometer uses a submillimeter laser, pumped by a CO_2 laser, as a local oscillator and a room temperature Schottky barrier diode as the first IF mixer. The radiometer can resolve spectral lines in the submillimeter region of the spectrum (arising from pure rotational molecular transitions) to within 0.3 MHz, using a newly developed acousto-optic spectrum analyzer which measures the power spectrum by simultaneously sampling 0.3 MHz wide channels over a 100 MHz bandwidth spanning the line. This report describes preliminary observations of eight spectral lines of H_2O_2, CO, NH_3 and H_2O, all lying in the 434–524 micrometer wavelength range; all eight lines were observed using two local oscillator frequencies obtained by operating the submillimeter laser with either methyl fluoride (CH_3F) or formic acid (HCOOH) as the lasing gas. Sample calculations of line parameters from the observed data show good agreement with established values. One of our development goals is the size and weight reduction of the package to make it suitable for balloon or shuttle experiments to detect trace gases in the upper atmosphere.

CONTENTS

INTRODUCTION

For the past several years an effort has been underway in the Instrument Electro-optics Branch of the Goddard Space Flight Center to develop a submillimeter heterodyne radiometer using a submillimeter laser as the local oscillator and a room temperature Schottky barrier diode as the first IF mixer.

The origins and development of this project are described in Reference 1; in this report we will give just a brief description of the experimental apparatus and an overview of the spectroscopic results obtained, with some analysis of the more significant spectroscopic measurements.

During the past year the radiometer has been used to make measurements in the laboratory of selected pure rotational lines of several molecules. These spectroscopic investigations have a three-fold purpose:

1. The main purpose is to demonstrate that the radiometer functions as intended -- that it is capable of producing high resolution spectral information with reasonable integration times. The accuracy of the spectral data is assessed by comparing it with independently known results.

2. The second purpose involves astronomical investigations of planetary atmospheres and the composition of interstellar nebulas. Such work is currently underway at Goddard; this instrument has been used with the NASA three meter infrared telescope at Mauna Kea, Hawaii for studies of the Orion nebula, under the direction of scientists from the Infrared and Radio Astronomy Branch. The spectral data obtained in the laboratory are useful in interpreting the results of these field experiments.

3. A third objective of the investigations is the support of upper atmosphere research, especially studies of the formation and breakdown of ozone. The radiometer should be able to detect trace amounts of various gases involved in these processes. Laboratory spectroscopic data are needed for both the design and analysis of such experiments, because

the atmospheric transmission problem must be solved for both the simulation of observations (to determine detectability) and the inversion of actual observations (to retrieve actual constituent concentrations). Spectroscopic data at submillimeter wavelengths do not generally exist; instruments of the type described in this report are the only existing means of acquiring the needed high resolution data.

Preliminary measurements have been made on selected spectral lines of H_2O_2, CO, NH_3 and H_2O; these are listed in Table 1.

Table 1
Spectroscopic Lines Investigated

Molecule	Line-Center Frequency (MHz)	Quantum Transition	Pressure Range (mtorr)	Receiver Noise Temperature (K)
H_2O_2	599,723.63 ± 0.1	9(0,9) ← 9(1,9)	300	
H_2O_2	601,885.28 ± 0.1	11(0,11) ← 10(1,9)	5 - 1,800	5,000
H_2O_2	603,394.93 ± 0.1	8(1,8) ← 8(0,8)	50 - 2,400	6,000
H_2O_2	606,717.54 ± 0.1	7(1,7) ← 7(0,7)	5 - 1,800	5,000
H_2O_2	608,865.	21(3,19) ← 22(2,21)	300 - 1,800	8,000
CO	691,472.97 ± 0.1	J = 5 ← 6	2 - 1,600	10,000
NH_3	572,498.15 ± 0.15		5 - 650	20,000
H_2O	620,700.81 ± 0.39		1,000	25,000

These lines all arise from pure rotational or rotational-torsional transitions in the vibrational ground state. The line-center frequencies are taken from Reference 2, with the exception of the 608865 MHz line of H_2O_2, for which the line-center frequency given above was measured in our laboratory. The frequencies measured in our laboratory for the other lines agree with the values in Table 1 to within a few MHz in most cases; this is quite good agreement, considering that frequency measurement was not a primary aim in our experiments. For the 608865 MHz line, the value given

in Reference 2 was calculated from theory; it differed from our measured value by several hundred MHz.

For each of the lines studied, the nearest neighboring lines (according to Reference 2) are separated from the line investigated by more than 1,000 MHz. Since the largest bandwidth of any of the spectrum analyzers used is about 300 MHz, it is clear that each of the lines studied is effectively isolated; i.e., not overlapped by any neighboring lines.

The range of sample cell pressures used allowed observations of the lineshape in both the doppler and pressure-broadened regimes, for some of the lines.

From the preliminary data obtained with the heterodyne radiometer and from comparisons of some of the data with theoretical results it was found that:

1. The radiometer is capable of actually achieving resolution to better than the doppler width; the best resolution to date is 300 KHz.

2. The radiometer is capable of giving the kind of laboratory spectroscopic data required for the design and analysis of upper atmosphere experiments.

3. Comparison of the radiometer data with some theoretical results and with previously known data showed good agreement.

EXPERIMENTAL APPARATUS

The absorption line to be observed is produced by directing the radiation from a hot blackbody source through a long cylindrical sample cell filled with the absorbing gas at low pressure. It is also possible to produce an emission line by replacing the hot source by a cold background; for example, an absorbent material cooled in liquid nitrogen.

The first heterodyne stage is a quasi-optical arrangement which translates the spectral line(s) being observed from the submillimeter region of the spectrum down to the microwave region. The local oscillator is a submillimeter laser, optically pumped by a CO_2 laser. The nearly monochromatic output of the submillimeter laser is optically combined in a diplexer with the beam emerging from the sample cell. The combined beam is then focused onto the whisker antenna of The Schottky diode mixer, which produces a down-shifted spectrum in the microwave region (18 GHz maximum).

The second heterodyne stage is a conventional microwave mixer which shifts the absorption line spectrum further down into the frequency range from 0.1 to 1 GHz (depending on the type of spectrum analyzer used), where it can be precisely measured.

The measurement of the spectral line, now in the sub-GHz region of the spectrum, is accomplished by observing it simultaneousiy in many channels, which span the width of the line. Two types of spectrum analyzers were used for this purpose: a conventional filter bank type and two different acoustooptic devices.

Details on the development and characteristics of the submillimeter laser local oscillator, the CO_2 pump laser, the diplexer, the Schottky diode mixer and related devices that make up the heterodyne receiver and data processing electronics are given in References 3-22. The laboratory apparatus is shown schematically in Figure 1.

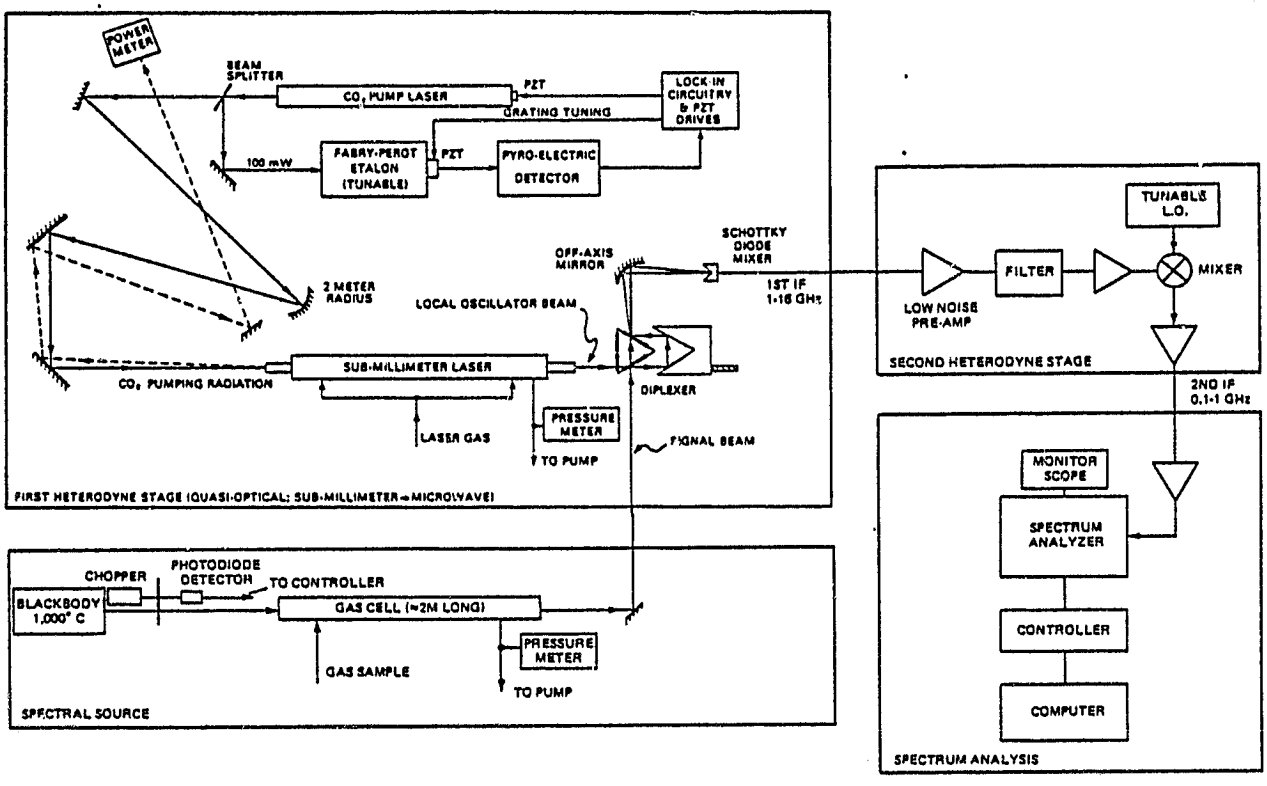

Figure 1. Submillimeter Wave Heterodyne Radiometer

The optical pump source for the submillimeter laser is an Apollo Model 550A 9-11 micrometer CO_2 flow-through laser using a CO_2-6%:N-18%:He-76% gas mixture (see Reference 1). For these experiments the CO_2 laser was operated at a pressure of 22 torr. The laser is presently capable of CW output up to 60w, but was operated at about 30w for these experiments. A cavity stabilizer PZT supplied by Apollo is used to maintain the pump line and under most experimental conditions a Burleigh etalon is used to lock on the pump wavelength to lend additional stability over long time periods. This is accomplished by monitoring a reflected beam from a ZnSe Brewster window located in the output beam of the laser. The Apollo has a diffraction grating with both horizontal and vertical adjustments to aid in locating and maximizing the required pump line. The CO_2 laser was calibrated with a spectrum analyzer to correlate the grating dial micrometer positions with pump lines in the 9 and 10 micrometer CO_2 branches.

The submillimeter laser cavity is the culmination of several years of design and construction

by N. McAvoy, G. Koepf, C. Rossey and C. Peruso (see References 1, 6, 10, 11, 13, 14, 21). The device is optically pumped by the Apollo CO_2 laser and is designed to function as a local oscillator in the 400-800 GHz (~750-375 μm) range. A 1.76 meter submillimeter cavity is used to produce an effective 14.08 m path length by reflecting the CO_2 beam on four round trips inside the cavity through the absorbing laser gas. The final reflection exits off-axis through the input port and is monitored by a pyroelectric power meter. The submillimeter laser beam is coupled through a 12mm quartz window at the exit port. There are adjustments for cavity wavelength and for internal mirror alignment external to the cavity, located at the exit end of the cavity. Maximizing the power of the unabsorbed CO_2 beam on the power meter is the technique used in making final alignment of the reflecting mirrors inside the submillimeter cavity. Bleed-in valves permit entry of a vaporized liquid from an external storage tube or direct entry of a gas simultaneously into the ends of the submillimeter cavity. Pressure in the cell is monitored near the middle of the cavity by a MKS baratron pressure gauge connected to a digital voltmeter (DVM). The cavity pressure ranges from about 30 to 150 mtorr, depending on the gas used. The design and operation of the submillimeter laser local oscillator and the CO_2 pump laser is given in greater detail in Reference 1.

A two meter glass cell made in-house serves as the sample cell. It is designed to accept gas samples directly or vaporize liquid samples from an external storage tube. A blackbody radiator serves as the source of energy for absorption. Although the blackbody produces a 1,300 K source, present indications are that optical coupling causes losses that result in an effective temperature difference of 250 K with respect to room temperature. Pressure in the cell is monitored near the exit port by a MKS baratron pressure gauge connected to a DVM. The blackbody radiation is chopped prior to entry into the sample cell at a variable rate dependent on the filter bank requirements.

The beam emerging from the sample cell and the submillimeter local oscillator beam are channeled into a diplexer (References 1, 9) which serves to combine the beams for input to the Schottky diode mixer. The diplexer is a Mach Zehnder interferometer, as shown in Fig. 2. A translator

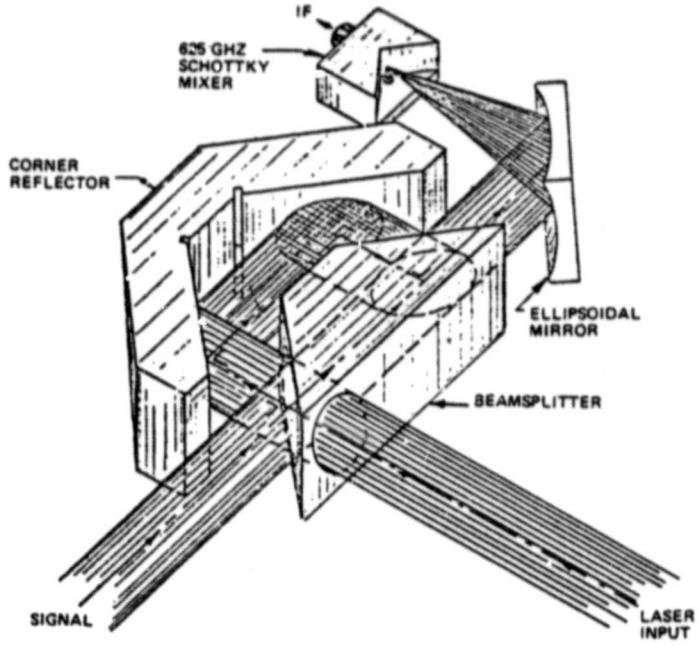

Figure 2. Mach-Zehnder Type Beam Diplexer

assembly on the diplexer permits adjustment of the reflective surface to tune the fringe pattern for constructive interference on the appropriate IF wavelength. This stage may also be used to accurately determine the wavelength of the submillimeter laser beam, since the interferometer spacing must also be an integral multiple of the submillimeter wavelength.

The mixer is a Schottky barrier diode designed and fabricated at Lincoln Labs for use as a receiver in our frequency range (see References 1, 3, 5, 7, 8, 12, 15, 16, 17, 19, 20). It is mounted in a corner cube and placed at the focus of an ellipsoidal mirror. The corner cube helps to match the diode antenna pattern to the submillimeter beams; it is mounted on a base with three degrees of translational freedom. A battery-powered bias box is used to provide a 0.07 ma current to the diode. A connection to an oscilloscope provides a monitor point for the submillimeter signal. This first IF signal is then fed into the second IF.

A low noise preamplifier and filter combination is used to boost the signal from the first IF. System noise temperatures are determined by matching of detectors to the low-noise preamplifiers.

Typical noise temperatures ranged from about 4,000 K to about 9,000 K. For the preliminary observations of NH_3 and H_2O, with extremely high first IF frequencies of about 12-16 GHz, the noise temperatures were in the 20,000-25,000 K range. If the first IF signal could be handled by the filter bank, as is the case for the conventional RF bank described later, then the signal was split: one channel going to the filter bank and the second channel to a crystal detector which was used to monitor the signal response from the sample. When one of the two acoustooptic spectrum analyzers was used, the first IF signal was downconverted by a second mixing stage (which uses a frequency synthesizer as the local oscillator) to the center frequency of the spectrum analyzer (either 150 MHz or 400 MHz). Double downconversion was necessary for H_2O and NH_3 because of the extremely high first IF's used. A DVM and a lock-in amplifier (referenced to the sample cell chopper) were used to monitor the second IF output signal. This set-up provides a means of determining the system noise temperature while running. The method of measuring the noise temperature is an adaptation of the so-called Y-method of system temperature measurement; it is described in detail in Reference 1.

Three different spectrum analyzers were used during these experiments: one conventional type using an RF filter bank and two acoustooptic analyzers. The conventional spectrum analyzer is described in Reference 23. It incorporates a second IF containing two tunable local oscillators, which together can accept RF signals up to several GHz and mix them up or down to the 1.170 GHz center frequency of the filter bank. This analyzer is designed to give 5 MHz resolution, using 64 channels. A block diagram is given in Figure 3.

The two acoustooptic spectrum analyzers (AOS's) both work on the same principle; functional diagrams (including the 2nd IF stage) are given in Figure 4. In both AOS's the spectral analysis is accomplished by using a Bragg cell. In this device high frequency sound waves, created by coupling the 2nd IF signal into a crystal by means of a piezoelectric transducer, create within the crystal a periodically varying index of refraction along the direction of propagation of the sound waves, caused by the density variations. This grating-like pattern causes an incident

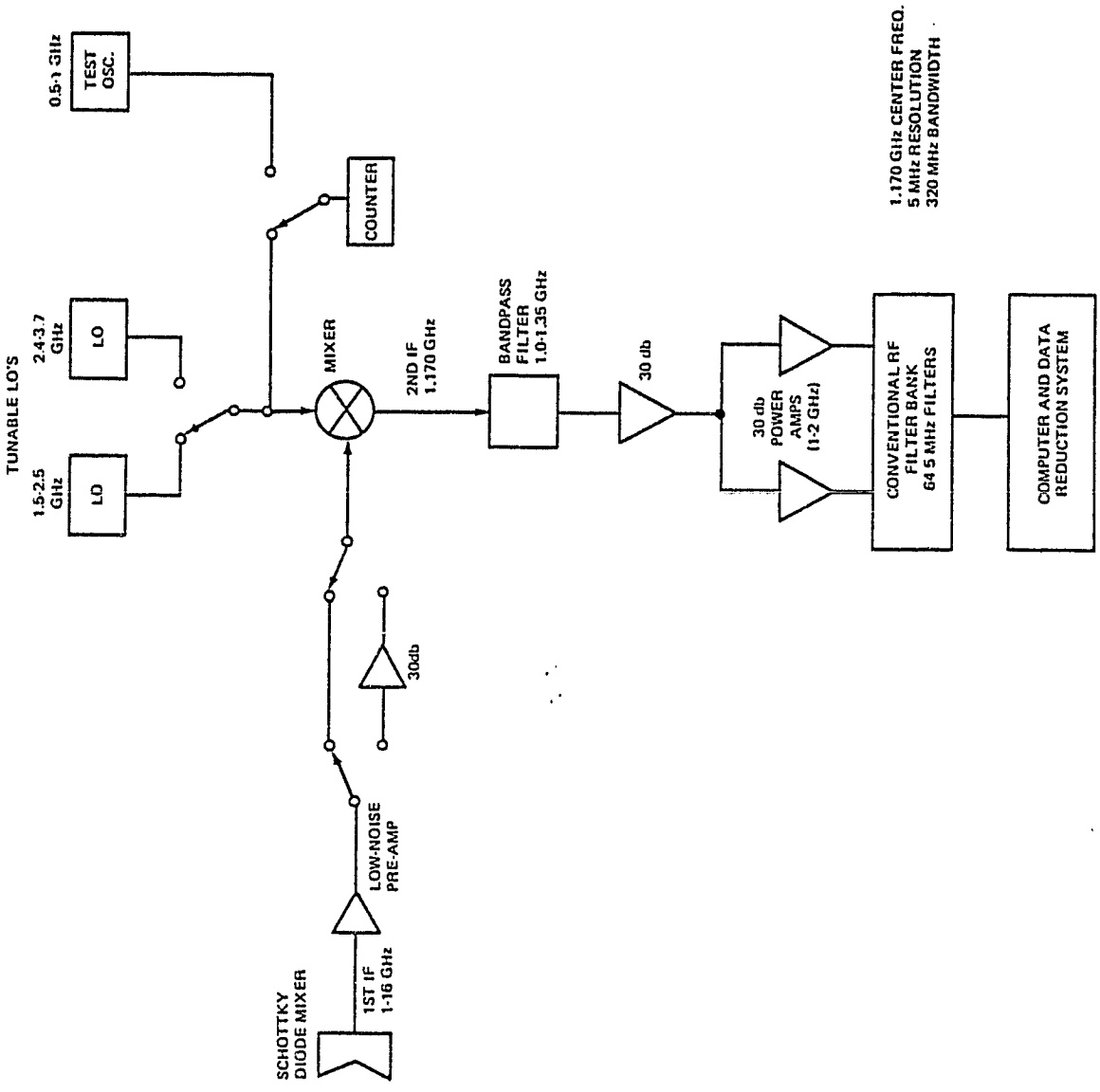

Figure 3. Conventional RF Filter Bank, Incorporating Second Heterodyne Stage

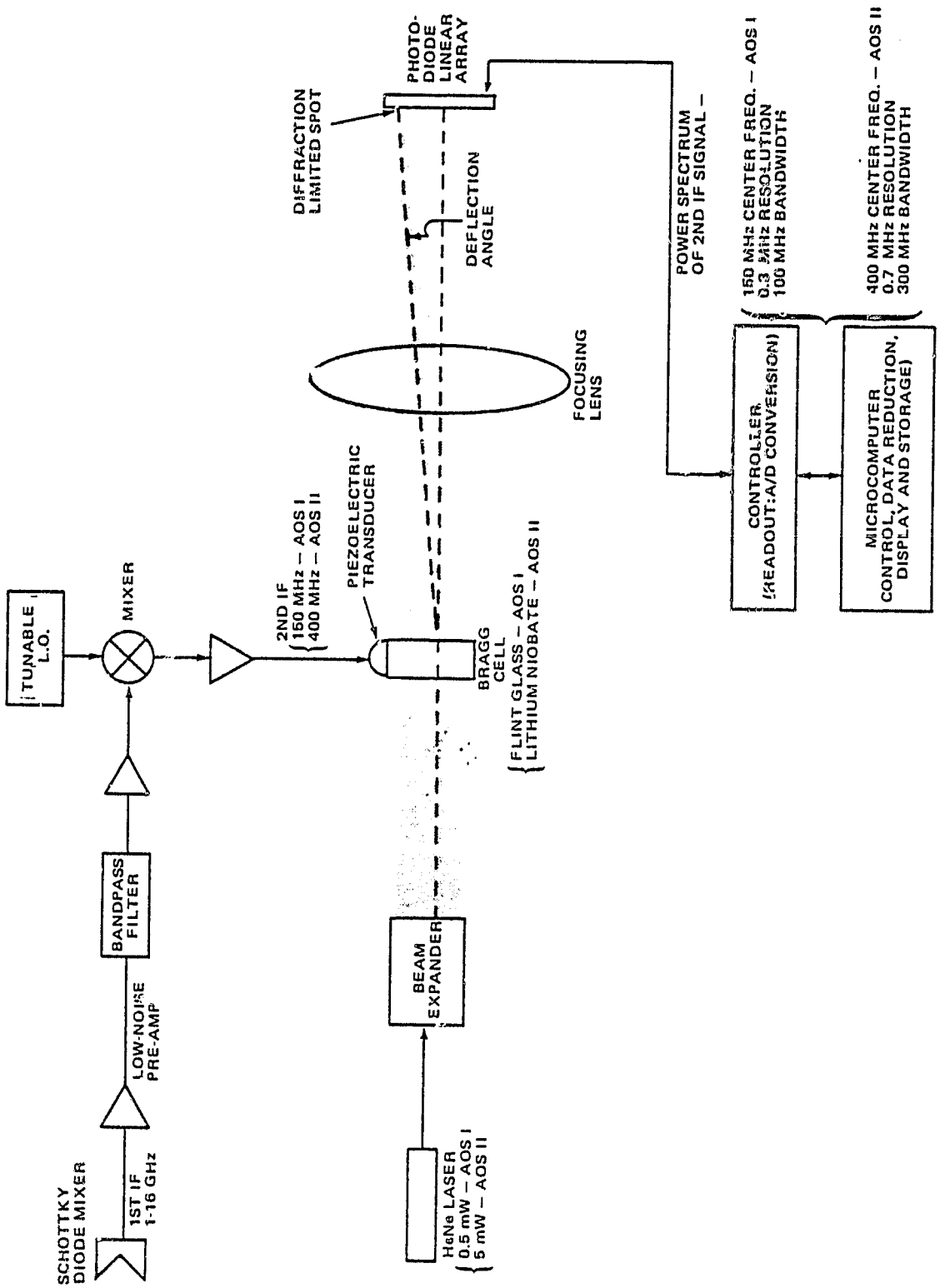

Figure 4. Acoustooptic Spectrum Analyzers (AOS I, II)

monochromatic light beam (from a HeNe laser) to be deflected through a small angle, the amount of deflection depending on the frequency of the 2nd IF signal. Since the signal contains a (band-limited) continuum of frequencies, the laser beam is spread out into a fan-shaped beam whose intensity varies with the deflection angle; in fact, the intensity is proportional to the amplitude of the corresponding signal frequency, so that the beam actually forms the spectrum of the 2nd IF signal. A lens then focuses the beam onto a linear array of integrating photodiode detectors; the output from these yields the signal power spectrum, with a finite resolution depending on the number of photodiodes. (The attainable resolution, and thus the number of diodes used, depends on the size of the diffraction-limited spots focused onto the diodes and on the angular spread of the deflected beam.) The theory and design of acoustooptic devices are given in References 24-28.

The two AOS's differ in the material used for the crystal (flint glass and lithium niobate for AOS I and II, respectively) and in design details. Functional diagrams for the two analyzers are shown in Figure 4; Figures 5 and 6 show a functional sketch and a photograph, respectively, of AOS I. AOS I was developed by the Instrument Electro-Optics Branch and AOS II by the Infrared and Radio Astronomy Branch; a more detailed description of AOS II is given in Reference 29. Each of the three spectrum analyzers has its own associated data collection and reduction system, as indicated in the figures.

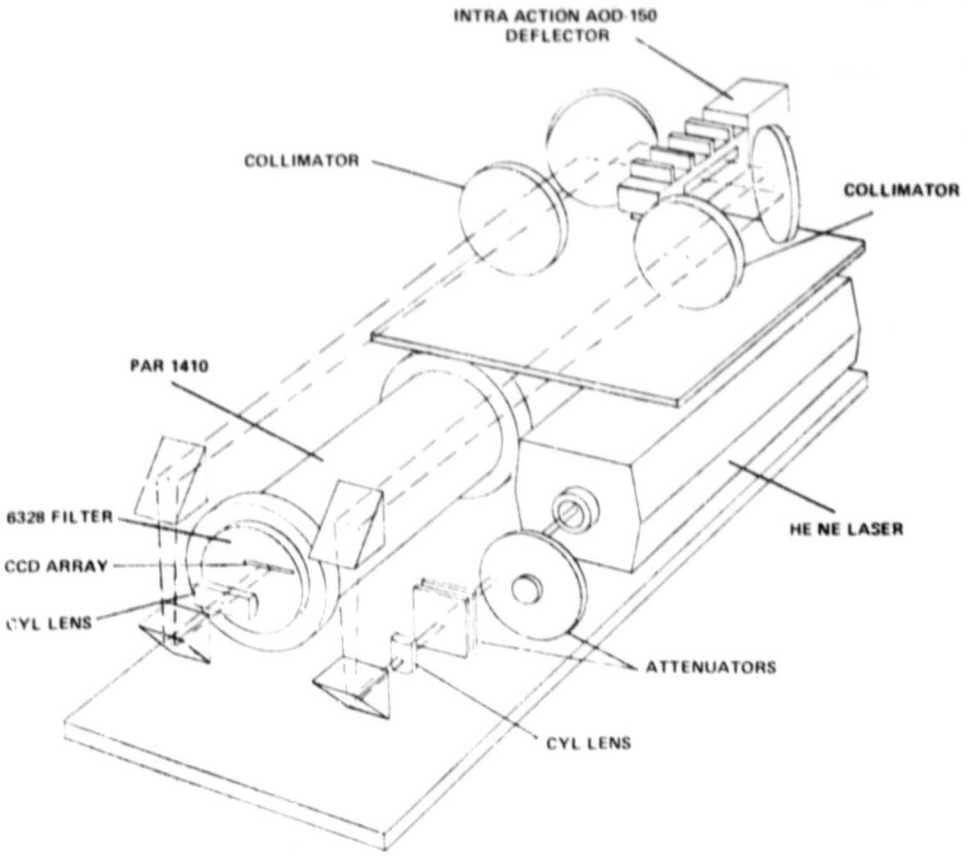

Figure 5. Sketch of AOS I

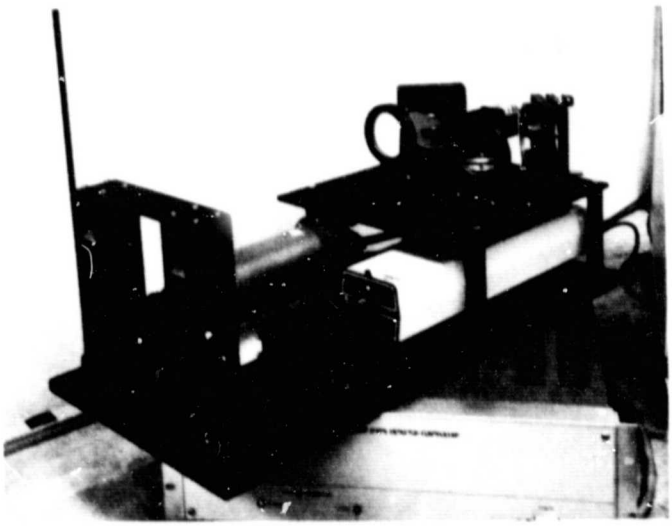

Figure 6. Photograph of AOS I

LABORATORY TECHNIQUE

Hydrogen peroxide (H_2O_2) and water (H_2O) samples were in liquid form. The liquid was placed in the external storage tube on the sample cell. The sample cell was evacuated to a reading on the pressure gauge which did not change and was calibrated to be 0 mtorr pressure. The entry port on the sample cell was opened and a sample pressure greater than required was noted. The entry port was closed off and the evacuation of the sample down to the desired pressure was observed on the pressure gauge. At this point the exit port of the sample cell was closed off. For carbon monoxide (CO) and ammonia (NH_3) cylinders of gas were hooked up to the exit port of the sample cell. An excess pressure was added to the sample cell, then the excess was removed while monitoring the pressure gauge. It should be noted that, as the desired pressure was approached, the bleed-off speed was slowed considerably to reduce any major gradient effects inside the sample cell after reaching the desired pressure. The run was made, then the sample cell was evacuated to 0 mtorr and an evacuated cell run was made. This technique was used to help make the measurements independent of the receiver noise temperature, as described in the Appendix.

Two submillimeter laser gases were used in these experiments: methyl fluoride from a gas cylinder and formic acid from a liquid storage tube. It was noted earlier that the gas line into the submillimeter laser is split, providing gas entry simultaneously at both ends of the cavity. When using methyl fluoride the evacuated cavity was brought to a pressure of about 40 mtorr of methyl fluoride, then the pressure was increased by about 50 mtorr by the addition of a buffer gas, sulfur hexafluoride. There are twin entry valves; each valve was connected to a gas cylinder. Liquid formic acid was placed in a glass storage tube which was connected to one of the entry valves. A pressure of about 80 mtorr was used for this laser gas.

Depending upon the strength of the line observed, integration times of 1.5 to 3 minutes were used during the data collection runs. It has been noted that a signal run was made followed by an evacuated cell run. The software associated with the data reduction, on either data system, permitted results to be plotted with normalization by the evacuated cell run. Any adjustments to the

system optics or electronics were made prior to a new run, not between the signal and evacuated cell runs. During these runs the CO_2 laser and the submillimeter laser remained quite stable, due in large measure to the stable room temperature of about 22 C. It was generally not necessary to use the Fabry-Perot etalon lock-in servo loop to maintain CO_2 pump amplitude and frequency stability.

SOME THEORETICAL BACKGROUND MATERIAL NEEDED TO REDUCE THE OBSERVED DATA TO LINE STRENGTHS AND WIDTHS

Relation Between the Observed Data and the Absorption Coefficient

The first step in reducing the data is to calculate the absorption coefficient α from the measured quantity, which we will call Q. (Q is a function of the signal and reference voltages at the output of the spectrum analyzer, as defined below.) A careful analysis of the processing of the input signals through the radiometer leads to the following relation (see the Appendix for a derivation):

$$\alpha(\epsilon) = \frac{1}{\ell} \ln \frac{1}{2Q(\epsilon)-1} \tag{1}$$

where the measured quantity Q is defined as:

$$Q = \frac{(S-R)/R}{(S_0-R)/R} \tag{2}$$

and α is the absorption coefficient in cm^{-1}, ℓ is the length of the gas sample cell in cm, ϵ is the frequency deviation from the line-center frequency, R is the voltage v measured at the output of the spectrum analyzer (for a given frequency interval, the width of which depends on the resolution of the spectrum analyzer) when the detector sees a reference source at some temperature (in our case, usually a chopper blade at room temperature), S is the same voltage when a signal is present (i.e., an absorption or emission line seen by the detector through the gas-filled cell) and S_0 is the same quantity, with the cell evacuated. To retrieve the signal (the spectral line) from the accompanying noise, the quantities S, S_0 and R are digitally integrated in the minicomputer associated with the spectrum analyzer.

It is important to note (see Appendix) that Eq. 2 leads to Eq. 1 only if the elapsed time between the measurements of S and S_0 is small enough so that there are no significant drifts in the gain or loss factors associated with the detector, or in the noise temperature of the detector. Note also that Q is unchanged by any linear transformation of v (i.e., $v' = av + b$); thus Q is unchanged by changes in the scale factor or zero point of the output voltages from the spectrum analyzer.

After the absorption coefficient $\alpha(\epsilon)$ has been obtained from the measured data $Q(\epsilon)$ with the help of Eq. (1), we try to obtain from $\alpha(\epsilon)$ what information we can on the line strength and width. To do this we need explicit formulas for $\alpha(\epsilon)$. These are collected below.

General Formula for the Absorption Coefficient (for a Single Gas)

The formula for the absorption coefficient for a given line has the following general form:

$$\alpha(\epsilon;p,T) = S(T)\cdot p\cdot g(\epsilon;p,T) \tag{3}$$

where S(T) is the line strength per unit pressure (i.e., the integrated absorption coefficient over the line width, per unit pressure), T is the absolute temperature, p is the pressure (assuming only a single gas) and g is the normalized line shape (described below). (Detailed derivations of these formulas may be found in References 30-32.)

Formulas for the Lineshape

The lineshape $g(\epsilon;p,T)$ is normalized so that the integral of g over the frequency width of the line is unity. The expressions for g for the different regimes may be put in the following forms:

For pure doppler broadening (Gaussian shape):

$$g_d(\epsilon;p,T) = \left(\frac{\ln 2}{\pi}\right)^{1/2} \frac{1}{\Delta_d(T)} e^{-\ln 2\left(\frac{\epsilon}{\Delta_d(T)}\right)^2} \tag{4}$$

where Δ_d is the half-width of the doppler-broadened line. It is given by the formula:

$$\Delta_d(T) = \frac{1}{c}\,(2\,kN_0\,\ln 2)^{1/2}\,\nu_0\left(\frac{T}{M}\right)^{1/2} \tag{5}$$

where k is Boltzmann's constant (numerical values and units are given below), N_0 is Avogadro's number, ν_0 is the line-center frequency and M is the molecular weight of the absorbing gas.

For pure pressure broadening (Lorentz form):

$$g_l(\epsilon;p,T) = \frac{\Delta_l}{\pi(\epsilon^2 + \Delta_l^2)} \tag{6}$$

where Δ_l is the half-width of the pressure-broadened line. It may be expressed in the form:

$$\Delta_l = p \cdot \Delta_0(T) \tag{7}$$

where Δ_0 is the linewidth for unit pressure. Usually the calculation of Δ_l (or Δ_0) from theory is very difficult and can only be done approximately; consequently it is necessary to resort to experimentally measured values of Δ_l. However, it is known that $\Delta_0(T)$ varies with T as $1/T$, for a long-range intermolecular force law (see Ref. 30, page 369).

For combined doppler and pressure broadening:

$$g_{comb}(\epsilon;p,T) = \left(\frac{\ln 2}{\pi^3}\right)^{1/2} \frac{p\,\Delta_0}{\Delta_d} \int_{-\infty}^{\infty} \frac{e^{-\ln 2 \left(\frac{\epsilon - t}{\Delta_d}\right)^2} dt}{(t^2 + p^2\,\Delta_0^2)} \tag{8}$$

where t is a variable of integration with the dimensions of frequency (sec^{-1}).

General Formula for the Line-Center Absorption Coefficient

The formula for the lineshape with combined doppler and pressure broadening is not analytically tractable, it may however be cast in various forms suitable for numerical computations (see, for example, Reference 31). For the special case of absorption at the line center ($\epsilon = 0$), the formula may be put in a particularly simple form in which the definite integral reduces to the probability integral. To derive this form we use the following definite integral evaluation:

$$\int_0^{\infty} \frac{e^{-\mu^2 x^2}}{x^2 + \beta^2}\, dx = [1 - \Phi(\beta\mu)] \frac{\pi}{2\beta}\, e^{\beta^2 \mu^2}$$

where $\mathrm{Re}\,\beta > 0$ and $|\arg \mu| < \pi/4$ (see Reference 33, page 338, formula # 3.466) and Φ is the probability integral:

$$\Phi(x) = \frac{2}{\pi^{1/2}} \int_0^x e^{-t^2}\, dt$$

If we apply this representation to Eq. 8, with $\mu = (\ln 2)^{1/2} / \Delta_d$ and $\beta = p\Delta_0$, we obtain the following expression for the line-center absorption coefficient:

$$\alpha(0;p,T) = \frac{1}{\pi^{1/2}\Delta_0} S(T) \, x \, e^{x^2} \, (1 - \Phi(x)) \tag{9}$$

where x, which is essentially the ratio of the collision width to the doppler width, is proportional to the pressure:

$$x = (\ln 2)^{1/2} \frac{p \, \Delta_0}{\Delta_d} = (\ln 2)^{1/2} \frac{\Delta_l}{\Delta_d} \tag{10}$$

This formula holds for all x (i.e., all pressures).

The probability integral may be calculated from the series representation

$$\Phi(x) = \frac{2}{\pi^{1/2}} \left(x - \frac{x^3}{3.1!} + \frac{x^5}{5.2!} - \frac{x^7}{7.3!} + \cdots \right) \tag{11}$$

which is convergent for all x but conveniently calculable only for $x \ll 1$, or from the series

$$\Phi(x) = 1 - \frac{e^{-x^2}}{\pi^{1/2} \, x} \left(1 - \frac{1}{2x^2} + \frac{1.3}{(2x^2)^2} - \frac{1.3.5}{(2x^2)^3} + \cdots \right) \tag{12}$$

which is semiconvergent for $x \gg 1$. For values of x near unity, tables of Φ may be used.

Equation 9 may be used to calculate the line strength S from experimentally measured values of the line-center absorption coefficient $\alpha(0; p_0, T_0)$ at pressure p_0 and temperature T_0. Note however that the pressure broadening parameter Δ_0 must also be known – probably from experimental observations, since it is difficult to calculate accurately from theory.

Formulas for the Line Strength

The calculation of the line strength from theory can be very difficult, depending on the molecule, and only order-of-magnitude estimates may be obtainable. The theoretical expression for the line strength may be put in the following general form:

$$S(T) = \frac{8\pi^3}{3c \, h \, k \, T} (1 - e^{-h\nu_0/kT}) \, f_l \, (T) \, \nu_0 \, | \mu_{ij} |^2 \tag{13}$$

where h is Planck's constant, ν_0 is the line-center frequency, f_l is the fraction of molecules in the lower state of the transition and μ_{ij} are matrix elements related to the dipole moment of the

transition. The difficulty lies in calculating f_1 and $|\mu_{ij}|^2$. Some general results are available, however (see, e.g., Ref. 30). For example, we may state the following results:

1. For diatomic (or linear) molecules, for pure rotational transitions in the υth vibrational state and for low J-values (J is the rotational quantum number):

$$f_1 \cong \frac{2J+1}{2(J+1)} \frac{h\nu_0}{kT} f_\upsilon \tag{14}$$

and

$$|\mu_{ij}|^2 \cong \frac{J+1}{2J+1} \mu^2 \tag{15}$$

where f_υ is the fraction of molecules in the υth vibrational state ($\upsilon = 0$ for the ground state) and μ is the dipole moment of the transition (see Ref. 30, Chapter 1). It follows that:

$$f_1 |\mu_{ij}|^2 \cong \tfrac{1}{2} \frac{h\nu_0}{kT} f_\upsilon \mu^2 \tag{16}$$

for these types of transitions in diatomic or linear molecules. In particular, $f_\upsilon \cong 1$ for the ground vibrational state at ordinary temperatures, so that for transitions within the ground state

$$f_1 |\mu_{ij}|^2 \cong \tfrac{1}{2} \frac{h\nu_0}{kT} \mu^2 \tag{17}$$

2. For symmetric-top molecules, for pure rotational transitions within the ground vibrational state and for low rotational quantum numbers (J and K),

   f_1 varies with T as $1/T^{3/2}$, approximately.

3. For transitions involving excited vibrational states, or for transitions between high-energy rotational levels of asymmetric- top molecules, the temperature dependence of f_1 is more complex.

If a good theoretical estimate of the line strength is not available, we must resort to an experimental measurement. If the line strength is strongly temperature dependent this would require measurement over the temperature range of interest. However we may find the line strength S(T) as a function of temperature from only a single measurement, provided we know the form of the function $f_1(T)$, expressed approximately as a power of T. For example, it is easy to derive formulas of the following type from Equations 3 and 13:

$$S(T) = \frac{\alpha(0;p_0,T_0)}{p_0 g(o;p_0,T_0)} \frac{T_0 f_1(T)}{T f_1(T_0)} \frac{1 - e^{-h\nu_o/kT}}{1 - e^{-h\nu_o/k T_o}} \tag{18}$$

This equation gives the temperature dependence of the line strength, provided we have an approximate expression for f_1 as a power of T, say T^a, because for this form the unknown coefficient of T^a will cancel. We need only measure the line center absorption coefficient $\alpha(0;p_0,T_0)$ at any convenient pressure p_0 and temperature T_0. In addition, we must use the lineshape function g which is appropriate; for example, if p_0 lies in the pressure-broadened regime, we must use g_l as given by Eq. (6), evaluated at $\epsilon = 0$, $p=p_0$ and $T=T_0$. Note that Eq. 18, once evaluated, applies to all pressure regimes, not just the one to which g applies. For example, if p_0 lies in the pressure-broadened regime, and we use g_l from Eq. (6), the resulting form of Eq. 18 applies to the doppler regime also. Note also that we may need, in addition to a measurement of α, a measurement of Δ_l, since the pressure broadening may not be accurately calculable from theory.

Condition for the Detectability of a Line

The minimum resolvable temperature difference of a radiometer of our type is given by the formula (see Reference 34, page 102):

$$(\Delta T)_{MIN} = \frac{(\pi/\sqrt{2})\, T_{SYS}}{(B\tau)^{1/2}} ,$$

where $(\Delta T)_{MIN}$ is the minimum detectable temperature difference (in K), T_{SYS} is the system noise temperature (the sum of the antenna noise temperature and the receiver noise temperature) referred to the antenna terminals (in K), B is the predetection bandwidth (in Hz) and τ is the post-detection integration time (in sec). If we interpret ΔT as the apparent line strength seen by the

detector, i.e., as the off-line temperature minus the line-center temperature, then the above formula relates the minimum detectable apparent line strength to the integration time, if B and T_{SYS} are regarded as constant.

Units and Constants

For all of the above equations the units and constants are as listed below.

Units

length	– cm
mass	– g
time	– s
charge	– statcoulomb
frequency	– Hz
temperature	– K
g	– s (or Hz^{-1})
α	– cm^{-1}
p	– $dyne/cm^2$
S	– s/g (or $cm^{-1} \cdot Hz \cdot (dyne/cm^2)^{-1}$)
μ	– statcoulomb-cm
M	– g/mol

Constants

c	$= 2.997925 \times 10^{10}$	cm/s	velocity of light in vacuo
h	$= 6.626196 \times 10^{-27}$	erg-s	Planck's constant
k	$= 1.380622 \times 10^{-16}$	erg/K	Boltzmann's constant
N_0	$= 6.022169 \times 10^{23}$	$mole^{-1}$	Avogadro's Number

Conversion Factors

1 joule = 10^7 ergs, exactly

1 debye = 10^{-18} statcoulomb-cm (dipole moment)

1 torr = 1.33322×10^3 $dyne/cm^2$

1 atm = 760 torr

LABORATORY MEASUREMENTS

H_2O_2 – 603.395 GHz

A local oscillator (LO) frequency close to 603 GHz was obtained by using methyl fluoride (CH_3F) as the lasing gas in the submillimeter laser. It produces the 604.2973 GHz line of CH_3F when optically pumped by the 9.55P20 line of the CO_2 laser. This scheme of submillimeter laser local oscillator operation was used for all H_2O_2 spectroscopy reported below. Mixing of the H_2O_2 line and the local oscillator frequency in the Schottky diode then produced a first IF signal at 902 MHz, which was analyzed on the conventional RF filter bank. Integration times of about 90 seconds were used on both the sample run and the evacuated cell run. Data was collected at the following sample pressures: 50, 100, 200, 300, 600, 900, 1200, 1500, 1800 and 2400 millitorr. System noise temperatures were about 6,000 K during the runs. An example of the spectra obtained is shown in Figure 7, for a pressure of 200 millitorr. Poor calibration of the vertical axis precludes any quantitative analysis, but it is clear from comparison of this spectrum with those taken at other pressures that the line is mostly pressure-broadened at 200 millitorr.

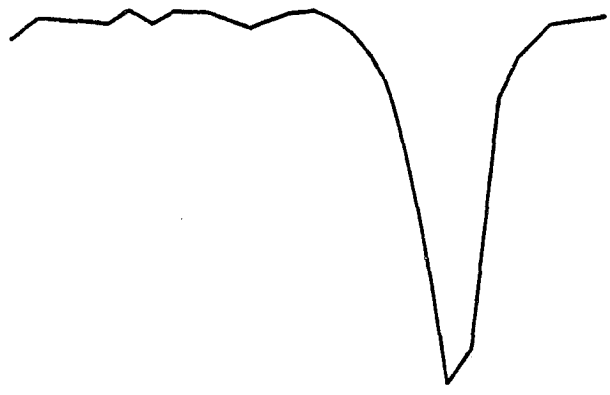

Figure 7. HOOH Line at 603 GHz, for 200 mtorr (RF filter bank)

H_2O_2 – 608.865 GHz

Mixing of the LO and sample beam produced a first IF frequency of 4.568 GHz, which was

amplified by a liquid nitrogen cooled amplifier. The output was sent to the conventional RF filter bank. Integration times of about 90 seconds were used for both the sample and evacuated runs. The following sample pressures were analyzed: 300, 600, 900, 1200, 1500 and 1800 millitorr. System noise temperature was about 8,000 K during testing. An example of the spectra obtained is shown in Figure 8, for a pressure of 300 millitorr. Again quantitative analysis is ruled out by poor vertical calibration and uncertainties in the pressure measurement, but it is clear from comparison of this spectrum with those taken at other pressures that the line is pressure-broadened at 300 mtorr.

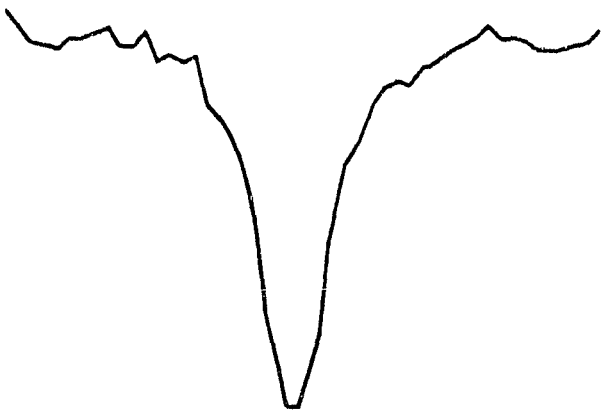

Figure 8. HOOH Line at 608 GHz, for 300 mtorr (RF filter bank)

H_2O_2 – 601.885 GHz, 606.717 GHz

The first time we studied these transitions we based the set-up on the 601.885 GHz line. The first IF signal of 2.412 GHz was sent directly to the conventional RF filter bank. Because of the double sideband conversion and the fact that the L.O. frequency of 604.297 GHz is nearly midway between the two H_2O_2 lines, the separation of the two lines after the first down-conversion

Figure 9. HOOH Lines at 601 and 606 GHz, for 900 mtorr (RF filter bank; lines not resolved)

(by the Schottky diode) was only about 8 MHz; these two lines were not resolved by the R.F. filter bank, which itself has a resolution of about 5 MHz. During this study the integration times were about 90 seconds. The pressures studied were: 300, 600, 900, 1200, 1500 and 1800 millitorr. The system noise temperature was about 5,000 K. An example of these spectra is shown in Figure 9; again quantitative analysis is ruled out by poor vertical calibration and uncertain pressure measurements, but again it is clear from comparison of this spectrum with those taken at other pressures that the lines are pressure-broadened at 900 mtorr.

During the second study of this pair of transitions the first IF signal of 2.412 GHz was down-converted by a second mixer to the 400 MHz IF used by the acoustooptic spectrum analyzer (AOS II). Integration times were about 70 seconds. The following pressures were studied: 5, 10, 20, 40, 80, 160, 320, 640 and 1,280 millitorr. System noise temperatures were about 5,000 K. It was with the AOS II resolution of 0.7 MHz that we were first able to verify the existence of both lines as suggested by the absorption results seen in the first study. Some of the spectra obtained are shown in Figures 10a-10f. The calibration for these spectra was good; some quantitative analysis is given in the section on analysis of data. It is clear from visual inspection of Figures 10a-10f that the two lines are mostly doppler broadened at 5 and 10 mtorr, although some pressure broadening is evident even at 10 millitorr. As the pressure increases the lines grow both deeper and broader (due to simultaneous doppler and pressure broadening) until they merge at around 100 mtorr. From this it is clear that the lines would not have been resolved in the first study even with greater resolution, unless measurements were made below 100 mtorr.

10a. 5 mtorr

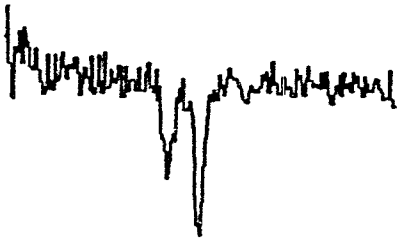

10b. 10 mtorr

10c. 20 mtorr

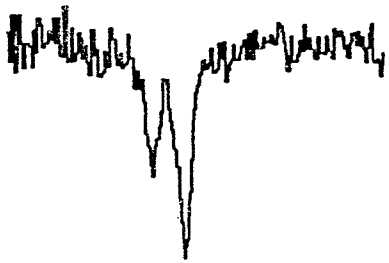

10d. 40 mtorr

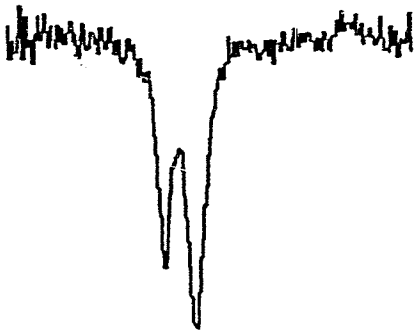

10e. 80 mtorr

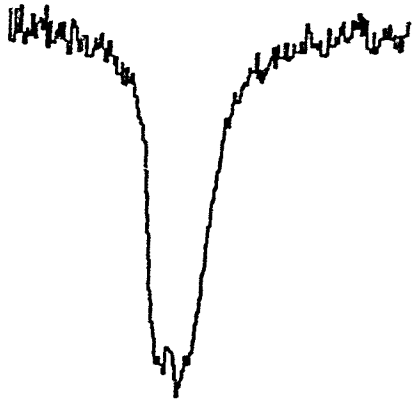

10f. 160 mtorr

Figures 10a - 10f. H_2O_2 Lines at 601 and 606 GHz, for 5-160 mtorr (AOS II; lines resolved, but merged at higher pressures)

CO – 691.473 GHz

A transition of J = 5←6 produces the 691.473 GHz line of carbon monoxide. A local oscillator frequency close to 691 GHz was obtained by using formic acid (HCOOH) as the lasing gas in the submillimeter laser, which produces the 692.9514 GHz line of formic acid when optically pumped by the 9.27R20 line of the CO_2 laser. This local oscillator frequency, when mixed with the sample beam, produces a first IF of 1.478 GHz. Three studies were made of this CO line using the same basic configuration.

The first study was done using AOS I. For this spectrum analyzer the first IF had to be downconverted to 150 MHz. Integration times up to several minutes were used. Pressures of 110, 220 and 300 millitorr were investigated. The system temperature in these early trials was about 9,000 K. Figure 11 shows one of the spectra, taken at 110 millitorr. These spectra were well calibrated, permitting some quantitative analysis; but this will not be given here, because the results of the third study are better (see the section on analysis of data). It is clear from comparison of the three spectra that the line is at least partially pressure-broadened at 110 mtorr.

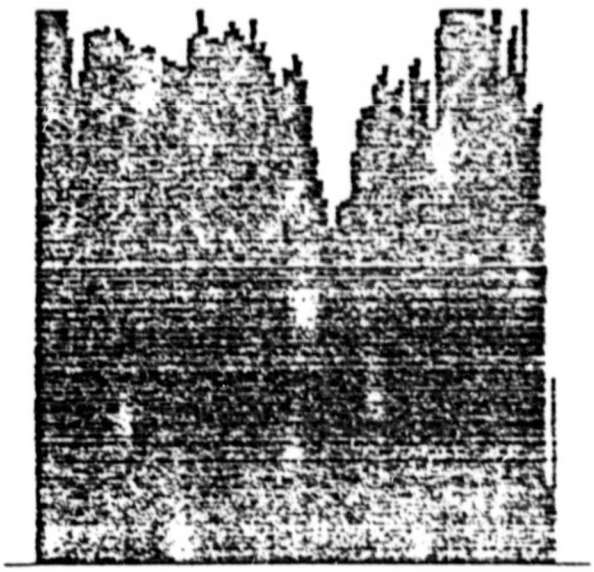

Figure 11. CO Line at 691 GHz, for 110 mtorr (AOS I)

The second study was done using AOS II. For this analyzer the first IF was downconverted to 400 MHz. Integration times of 70 seconds were used for both the sample

and evacuated cell runs. Pressures studied were: 60, 100, 300, 1,000 and 2,000 millitorr. The system temperature was about 4,000 K. Lack of calibration of the vertical axis precluded quantitative analysis of these spectra. An example is shown in Figure 12.

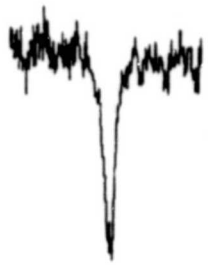

Figure 12. CO Line at 691 GHz, for 300 mtorr (AOS II)

The third study was done using AOS I, with an improved data collection and analysis system. Integration times of 80 seconds were used for all pressures except 2 mtorr, which required 160 seconds. Pressures of 2, 5, 10, 20, 50, 100, 200, 400, 800 and 1600 mtorr were investigated. Figures 13a-13j show these spectra. The data collection and analysis system was considerably improved for these investigations (see Reference 35), and the data are quite well calibrated. In the section on analysis of data these results are shown to yield a value for the dipole moment of CO (for the transition involved) which is quite close to the value given in the literature. It is worth noting also that the range of pressures goes from the doppler regime (or close to it) at the low end to the collision-broadened regime at the high end. Note that the frequency scales in all the plots in Figure 13 have been arbitrarily shifted to read 0 MHz near the line center. The actual frequency of the zero marker is noted on each plot; these frequencies were determined by prior calibration of the acoustooptic spectrum analyzer resolution elements with a sine wave generator.

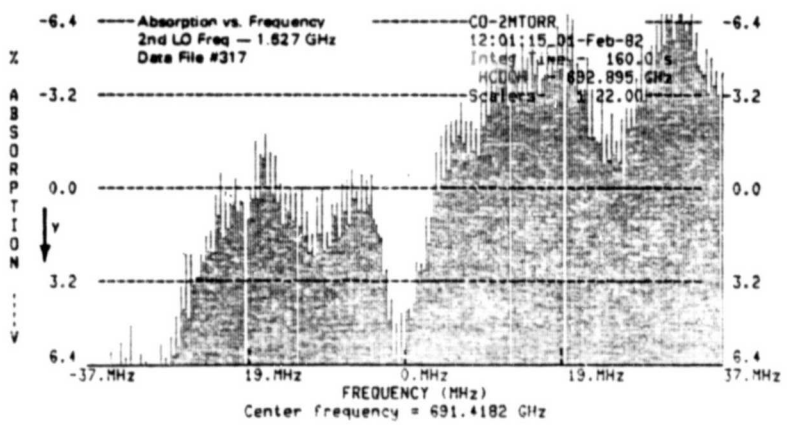

Figure 13a. CO Line at 691 GHz, for 2 mtorr

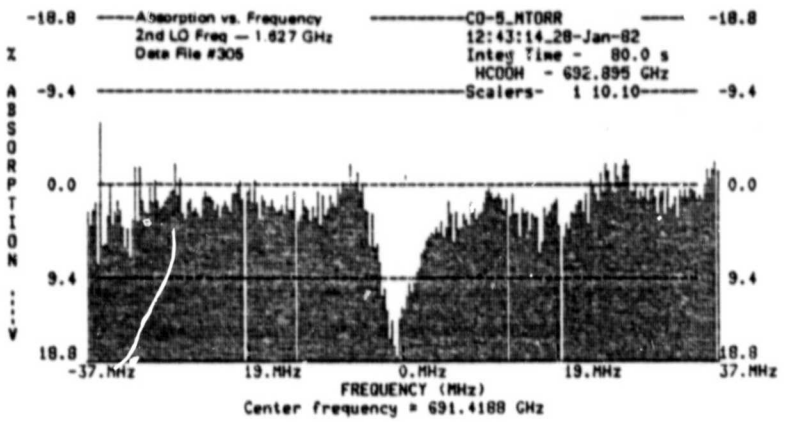

Figure 13b. CO Line at 691 GHz, for 5 mtorr

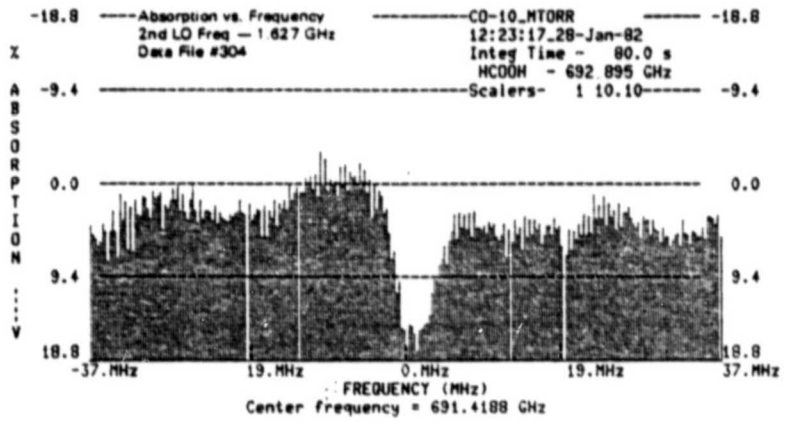

Figure 13c. CO Line at 691 GHz, for 10 mtorr

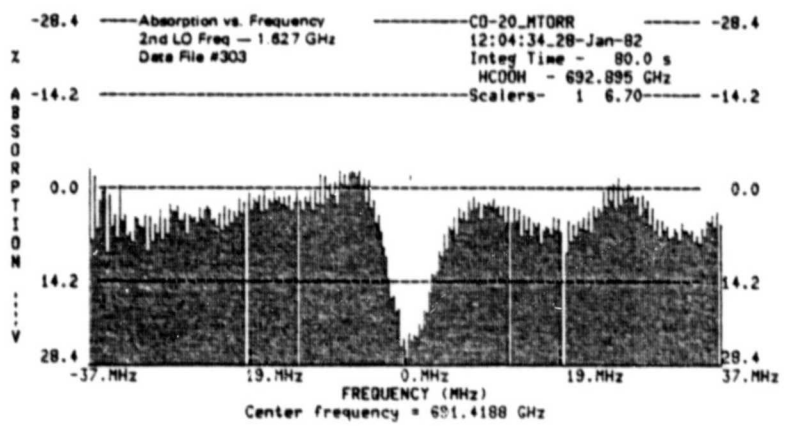

Figure 13d. CO Line at 691 GHz, for 20 mtorr

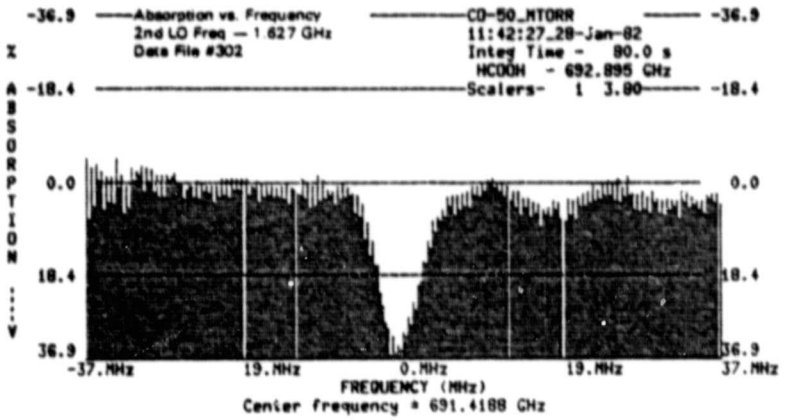

Figure 13e. CO Line at 691 GHz for 50 mtorr

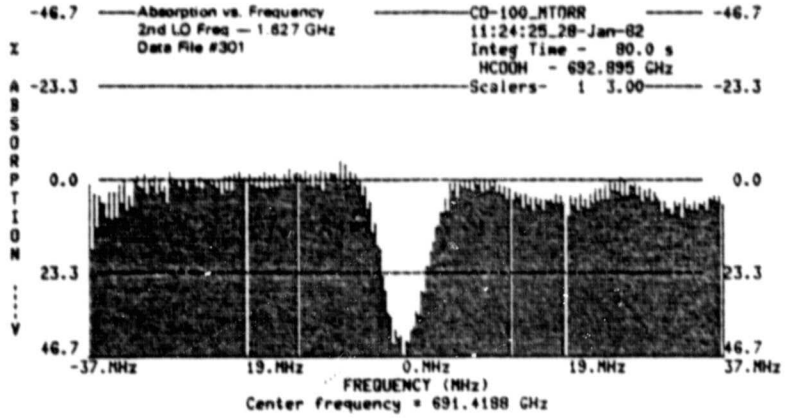

Figure 13f. CO Line at 691 GHz for 100 mtorr

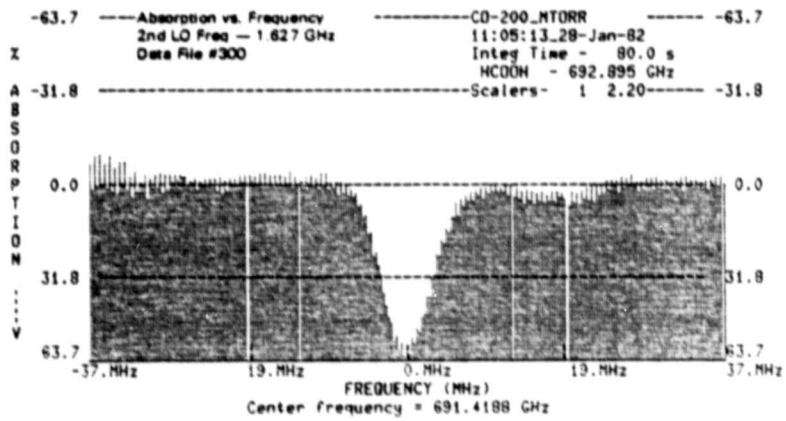

Figure 13g. CO Line at 691 GHz for 200 mtorr

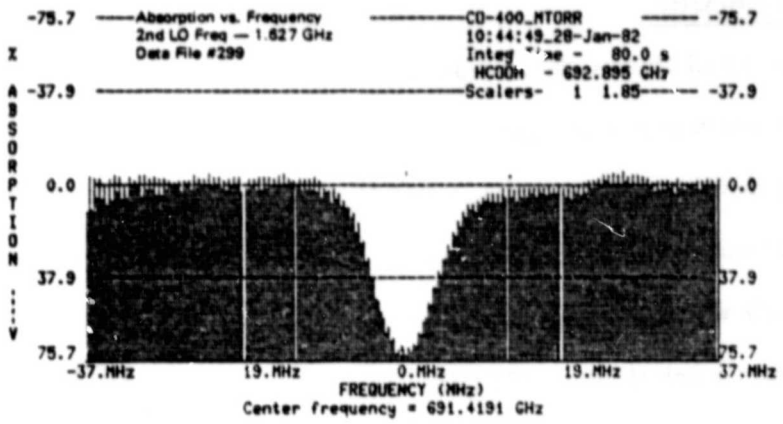

Figure 13h. CO Line at 691 GHz for 400 mtorr

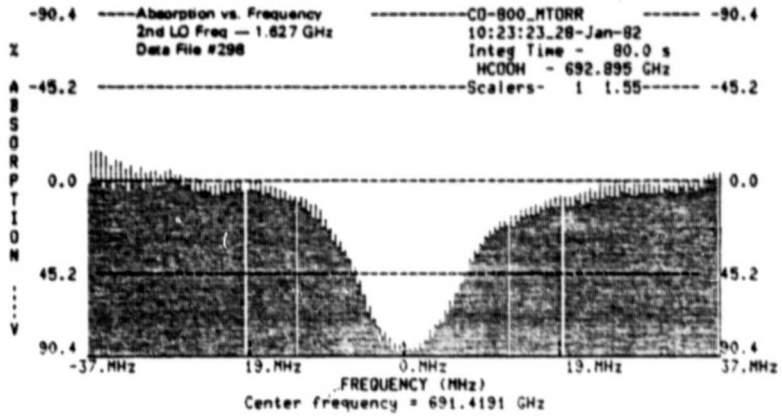

Figure 13i. CO Line at 691 GHz for 800 mtorr

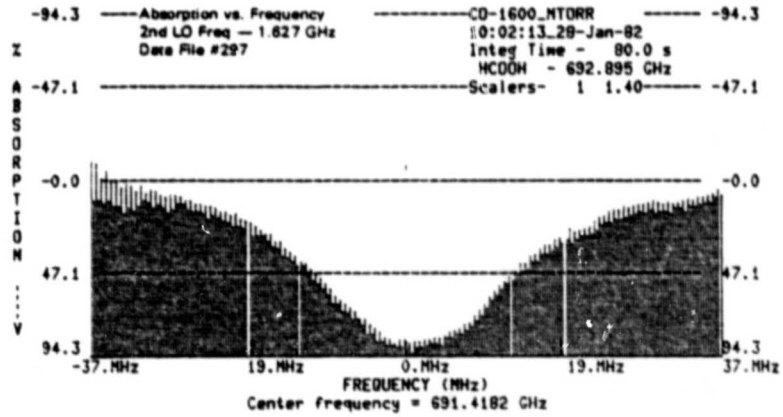

Figure 13j. CO Line at 691 GHz for 1600 mtorr

NH_3 – 572.498 GHz

We ran initial studies on the transition of ammonia which produces a line at 572.498 GHz. Using HCOOH pumped by the 9.23R28 CO_2 line, a local oscillator frequency of 584.3729 GHz was produced. Mixing at the diode produced a first IF of 11.875 GHz. Using a liquid nitrogen cooled preamplifier this signal was downconverted to the 400 MHz IF of AOS II. Integration times were about 180 seconds for both the sample run and the evacuated cell run. Pressures of 5, 10, 20, 40, 160 and 640 millitorr were studied. System noise temperature was about 20,000 K. For these spectra quantitative analysis was not an objective; the primary purpose was to verify that heterodyne techniques with a large IF (12 GHz) could produce usable spectra. Figure 14 shows an example of the spectra obtained.

Figure 14. NH_3 Line at 572 GHz, for 5 mtorr (AOS II)

H_2O – 620.701 GHz

Finally, a short study was done to see if the system could locate the transition of water which produces a 620.701 GHz line. Using methyl fluoride as the submillimeter laser gas, optically pumped by the 9.55P20 CO_2

line, a local oscillator frequency of 604.2973 GHz was produced. Mixing of this frequency with the H_2O line produced a first IF frequency of 16.403 GHz. Using a liquid nitrogen cooled preamp, this signal was down-coverted to 150 MHz by the mixers available at the time and then sent to the conventional RF filter bank, where the on-board mixer generated the 1.170 GHz signal it required. Integration times of 60-180 seconds were used for a pressure of 1,000 mtorr of H_2O. Movement of the second IF allowed tentative verification of the line, although no further tests were done. The system noise temperature was about 25,000 K. For these spectra quantitative analysis was not an objective; the primary purpose was once again to verify that heterodyne techniques with a large IF (16 GHz) could produce usable spectra. A sample spectrum is shown in Figure 15.

Figure 15. H_2O Line at 620 GHz, for 1000 mtorr (RF filter bank)

Emission Studies

There were additional tests to study the emission spectra of H_2O_2 and CO. For these tests the hot blackbody source was replaced with a piece of ecosorb dipped in liquid nitrogen. These preliminary results support the utility of the radiometer for emission studies. An example of these spectra is shown in Figure 16; it is an emission spectrum of the RQ0 9(0,9)←9(1,9) line of H_2O_2 at 599 GHz, taken at a pressure of 300 millitorr.

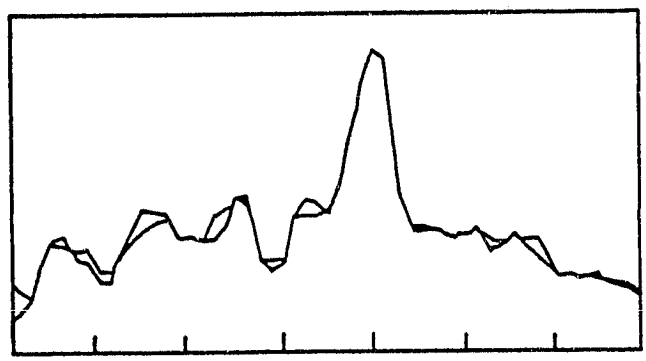

Figure 16. Emission Line of H_2O_2 at 599 GHz, for 300 mtorr (RF filter bank)

ANALYSIS OF DATA

The analysis of the data given below is intended to help assess the capability of the heterodyne radiometer, as presently set up, to yield the quality of spectroscopic data we will later need for the design and analysis of upper atmosphere and astronomy experiments.

To decide this question we will try to extract information on line strengths and widths from some of the spectroscopic data so far obtained, then compare this information with known values of these quantities for the observed lines. If the agreement is good enough, we could conclude that the heterodyne radiometer is able to measure the kind of spectroscopic data we will need. As will become evident from the following discussion, it turns out that the instrument is able to measure such data, but improvements are recommended.

CO – 691.473 GHz

For this line the first study, using AOS I, yielded a set of data which was reasonably well calibrated but spanned only the pressure range from about 100 to 300 mtorr. Because the data from the third study, using AOS I with an improved data collection and analysis system, had better frequency resolution (0.3 MHz as compared to 1 MHz) and spanned the pressure range from 2 to 1600 mtorr, only that data will be used in the analysis given below. The data from the second study, using AOS II, was not calibrated and so could not be analyzed.

The data from the third study yielded a value for the dipole moment of CO which agrees quite well with the value given in the literature. The analysis leading to this result follows.

From the plots of the absorption line at various pressures it is possible to read the line-center absorption coefficient and the linewidth at each pressure; the values thus found are given in Table 2.

Table 2.
Experimental Results from the Third Study of the CO Absorption Line at 691.473 GHz

Pressure (mtorr)	Line-Center Absorption Coefficient (cm^{-1})	Linewidth (MHz; HWHM)	Total Absorption (cm^{-1} MHz)
2*	0.00041	1.9	0.00078
5	0.0010	2.1	0.0021
10	0.00097	3.0	0.0029
20	0.0016	3.2	0.0051
50	0.0022	3.2	0.0070
100	0.0030	3.0	0.0090
200	0.0053	3.6	0.019
400	0.0074	4.6	0.034
800	0.012	6.9	0.083
1600	0.015	12.4	0.187

The linewidth is read directly from the plot; the line-center absorption coefficient is calculated from the ordinate y shown on the plot (labeled "% absorption") by the relation

$$\alpha = \frac{1}{\ell} \ln \frac{1}{2Q-1} = \frac{1}{\ell} \ln \frac{1}{1-y/100} \qquad (19)$$

where the first equation is just Eq. 1 (see the Appendix for a derivation) and the second equation expresses the absorption coefficient α in terms of the plot ordinate y, which is related to the measured quantity Q by $y = (1-Q) \times 200$. The length ℓ of the sample cell is 190.5 cm. The quantity called "total absorption" in Table 2 is the product of the line-center absorption coefficient and the linewidth; it is proportional to the area under the absorption line, which is the total absorption. This quantity should be proportional to the pressure for all pressures considered here. To better see the variation of the line-center absorption coefficient, linewidth and total absorption with

*This data point was measured in a separate experiment.

pressure, these three quantities are plotted vs. pressure in Figure 17. (The common ordinate in Figure 17 is just a relative scale, chosen so that all three quantities fit on the same plot; the three curves were just drawn freehand – no mathematical curve-fitting was done.)

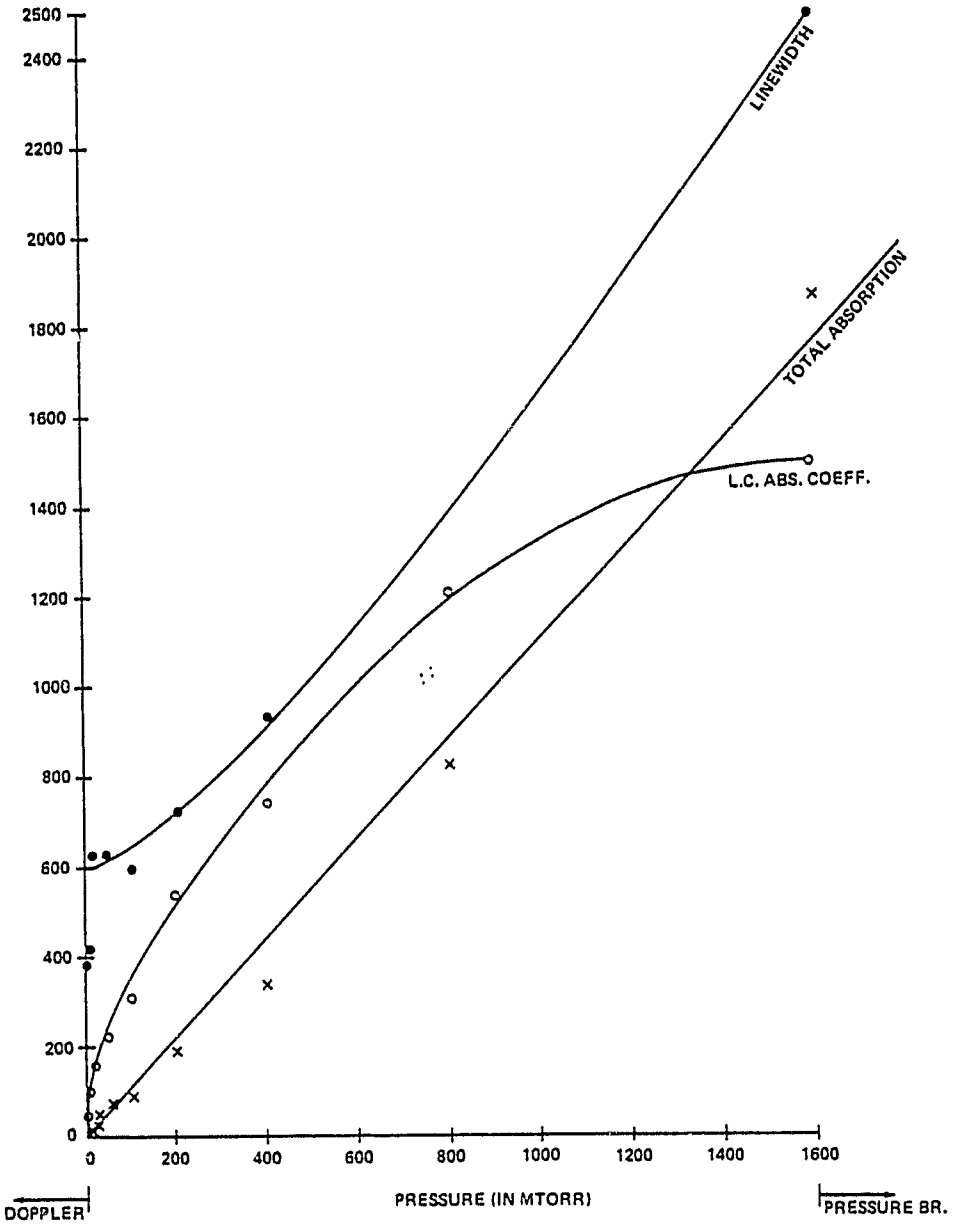

Figure 17. Variation of Line-Center Absorption Coefficient, Linewidth and Total Absorption with Pressure

From Figure 17 it is seen that the linewidth flattens out at the lower end of the pressure range and becomes linear at the high end, while the line-center absorption coefficient rises linearly at the low end and flattens out at the high end and the total absorption varies quite linearly with pressure through the entire range. (The two data points at 2 and 5 mtorr are apparently not as good as the others, and may be disregarded.) From the variation of these quantities with pressure it is apparent that the lower end of the pressure range approaches the doppler regime and the high end is in the pressure-broadened regime.

From the fact that the data point at 1600 mtorr is in the pressure-broadened regime it follows that we may compute the pressure-broadening coefficient Δ_0 from this data point with reasonable accuracy; we find:

$$\Delta_0 \text{ (300 K)} \cong 7.8 \text{ MHz/torr} \quad \text{(HWHM)} \tag{20}$$

where the 300 K figure refers to the fact that the gas in the sample cell is assumed to be at approximately room temperature (recall that Δ_0 depends on temperature). With this value of Δ_0 and the values of the line-center absorption coefficient given in Table 2 we may use Eq. 9 to compute the line strength S at T = 300 K. The only other quantity we need is Δ_d, the doppler halfwidth, which is needed to compute the values of x from Eq. 10; Δ_d is easily computed from Eq. 5, with T = 300 K and M = 28. We find:

$$\Delta_d \text{ (300 K)} = 0.81 \text{ MHz} \quad \text{(HWHM)} \tag{21}$$

If we regard the doppler region as defined by $\Delta_\ell = p\Delta_0 < 1/10\ \Delta_d$, then, using the value of Δ_0 found above, we find that the doppler regime holds for $p < 10$ mtorr. For p = 100 mtorr, $\Delta_\ell \cong \Delta_d$, so that for pressures less than about 100 mtorr the linewidth levels off and decreases slowly until $\Delta_\ell << \Delta_d$, below which it remains constant. From Table 2 it is evident that the linewidth does behave this way (although the numerical values, as might be expected, are not exactly consistent, probably due to errors in the measurement of pressure).

With the values of Δ_d and Δ_0 computed above we may use Eq. 10 to compute the x-values. Eq. 9 may then be used to compute the values of S(300K) from the values of the line-center absorption coefficient for the various pressures; the probability integral Φ may be obtained from tables or computed from one of the series expansions given above. The result of these calculations is a collection of values for S which range from 77 to 268 Hz cm^{-1} (dyne/cm^2)$^{-1}$. Since S is independent of pressure, the approximately 3.5 to 1 variation in these values of S appears to indicate experimental errors or shortcomings in the theoretical expressions, or both. In any case the variation is small enough to give us an order-of-magnitude estimate of S. We will therefore simply take the mean of the S-values and use it to compute the dipole moment. The mean is found to be:

$$S_{av}\ (300K) = 168\ \text{Hz cm}^{-1}\ (\text{dyne/cm}^2)^{-1} \tag{22}$$

To compute the dipole moment we use Eq. 13, where, for a diatomic molecule such as CO at ordinary temperatures, the quantity $f_l\ (T)\ |\mu_{ij}|^2$ is given by Eq. 17. The resulting relation is:

$$S(T) = \frac{4\pi^3 \nu_0^2}{3c(kT)^2}\left(1 - e^{-h\nu_0/kT}\right)\mu^2 \tag{23}$$

where μ is the dipole moment of the transition in statcoulomb-cm. If we set T = 300K, put in the values of the mathematical and physical constants (see the Theoretical Background section of this report) and express μ in debyes (1 debye = 10^{-18} statcoulomb-cm), we find:

$$\mu \cong 0.07 \quad \text{debye} \tag{24}$$

This value compares quite well with the value 0.1 debye given in the literature (see, for example, Reference 30). We may thus conclude that the experimental CO data yield a rather accurate value for the line strength of the transition.

H_2O_2 – 601.885 GHz, 606.717 GHz

For this pair of lines the second set of observations, using AOS II, yielded line strengths in order-of-magnitude agreement with theoretical values (Ref. 36).

The observations at 5 and 10 millitorr appeared to be in the doppler regime. From the observations at 5 millitorr (see Figure 10a), and using the formula

$$\alpha(0) = \frac{1}{\ell} \ln \frac{1}{2Q(0)-1} \tag{25}$$

(from Eq. 1, setting $\epsilon = 0$) to get the line-center absorption coefficient for each line, we found that:

$$\alpha(0) = 0.0012 \text{ cm}^{-1} \text{ for the 601 GHz line}$$

and (26)

$$\alpha(0) = 0.0028 \text{ cm}^{-1} \text{ for the 606 GHz line,}$$

where both absorption coefficients are for $p_0 = 5$ millitorr and $T_0 = 300$ K. If we now use Eq. 3 with $\epsilon = 0$, $p = p_0 = 5$ mtorr and $T = T_0 = 300$ K, we can write:

$$S_{EXP}(300K) = \frac{\alpha(0; p_0, T_0)}{p_0 \, g_d(0; p_0, T_0)} \tag{27}$$

for each line. We easily calculate that

$$\Delta_d(300K) = \begin{cases} 0.622 \text{ MHz (601 GHz line)} \\ 0.627 \text{ MHz (606 GHz line),} \end{cases} \tag{28}$$

$$g_d(0; p_0, T_0) = \begin{cases} 0.756 \times 10^{-6} \text{ Hz}^{-1} \text{ (601 GHz line)} \\ 0.750 \times 10^{-6} \text{ Hz}^{-1} \text{ (606 GHz line)} \end{cases} \tag{29}$$

and

$$S_{EXP}(300K) = \begin{cases} 238 \text{ cm}^{-1} \text{ Hz (dyne/cm}^2)^{-1} \text{ (601 GHz line)} \\ 560 \text{ cm}^{-1} \text{ Hz (dyne/cm}^2)^{-1} \text{ (606 GHz line).} \end{cases} \tag{30}$$

We now want to compare these experimental values of the line strength with the theoretical values from Ref. 36:

$$S^*_{TH}(300K) = \begin{cases} 0.1119 \text{ cm}^{-2} \text{ atm}^{-1} \text{ (601 GHz line)} \\ 0.2045 \text{ cm}^{-2} \text{ atm}^{-1} \text{ (606 GHz line)} \end{cases} \tag{31}$$

To make the comparison we must note that S* and our S do not differ merely in the units used, but are different quantities. S* is defined in terms of the wavenumber of the radiation, whereas S is defined in terms of the frequency. It is not difficult to derive the relation between the two quantities; it turns out to be:

$$S^*(T) = 0.338 \times 10^{-4}\ S \tag{32}$$

where the units of S* are $cm^{-2}atm^{-1}$ and the units of S are $cm^{-1}\,Hz(dyne/cm^2)^{-1}$. From Eq. 32 we may write the theoretical values in terms of S:

$$S_{TH}(300K) = \begin{cases} 3310\ cm^{-1}\ Hz\ (dyne/cm^2)^{-1} & (601\ GHz\ line) \\ 6050\ cm^{-1}\ Hz\ (dyne/cm^2)^{-1} & (606\ GHz\ line) \end{cases} \tag{33}$$

Comparison of these values with those given by Eq. 30 shows that the theoretical line strengths and the line strengths observed with the heterodyne radiometer are about an order of magnitude apart. Considering the necessarily approximate nature of the theoretical calculations for the H_2O_2 molecule, which is an asymmetric rotor, and the preliminary nature of the experimental observations, these results must be considered reasonably good.

Sensitivity of Radiometer

We can determine whether the radiometer is able to detect a small signal approaching the theoretical limit by comparing the signal strength of one of the weaker observed spectral lines with the minimum observable signal as calculated from the above equation. For this purpose we choose the CO line shown in Figure 13a, because at a pressure of 2 mtorr this line is approaching the noise level and the good calibration of the plot allows the signal level to be calculated.

To find ΔT from Figure 13a we must first relate ΔT to the ordinate y shown in the figure. This can be done by using Equations 19, A7 and A9; simple manipulation of these three equations yields the relationship we want:

$$\Delta T = \frac{1}{100}\left[(1-\beta)T_{BB} + \beta\, T_{GAS} - T_{REF}\right] y,$$

where T_{BB} is the temperature of the blackbody source, T_{GAS} is the temperature of the gas and T_{REF} is the temperature of the reference body (the chopper blade), all in degrees Kelvin. The factor β may be regarded as including losses in the sample cell and optical coupling losses resulting from mismatch between the beam incident on the whisker antenna of the Schottky diode detector and the antenna pattern; preliminary measurements indicate that $\beta \approx 0.8$.

From Figure 13a we see that $y \approx 5$ at the center of the absorption line; assuming that T_{BB} = 1,300 K, $T_{GAS} = T_{REF}$ = 300 K and β = 0.8, we find that ΔT = 10 K. Thus the radiometer in this case was able to clearly see an apparent temperature difference of ten degrees Kelvin. To compare this with the minimum detectable ΔT we note that an integration time of 160 seconds was used for the spectrum shown in Figure 13a; if we assume a noise temperature of 10,000 K and note that the predetection bandwidth is 0.3 MHz we find from the radiometer equation given on page 20 that $(\Delta T)_{MIN}$ = 3.2 K. Thus the radiometer was able in this case to clearly see a signal which is only three times the theoretically minimum detectable signal.

SUMMARY AND CONCLUSIONS

The heterodyne radiometer was used to study selected lines of four gases: hydrogen peroxide (H_2O_2), carbon monoxide (CO), ammonia (NH_3) and water (H_2O). All lines studied were in the frequency range 572-691 GHz, which corresponds to a wavelength range of 434-524 micrometers. Two gases were used in the submillimeter laser to obtain appropriate local oscillator frequencies: methyl fluoride (CH_3F) and formic acid (HCOOH). In all, eight lines were investigated. For three of these (a CO line and two H_2O_2 lines) the data were good enough to do some analysis, giving good agreement with theory. From the results obtained in these preliminary investigations it was concluded that the heterodyne radiometer is capable of being used for precise spectroscopic investigations in the laboratory in the submillimeter region of the spectrum, for both absorption and emission spectra.

The prospects are equally good for use of the heterodyne radiometer in astronomical investigations, particularly the detection of molecular species in interstellar nebulas. The radiometer was successfully used to detect the presence of CO in the Orion nebula by observing the J=5←6 transition at 691 GHz; these observations were made at the NASA Infrared Telescope Facility on Mauna Kea, Hawaii, at an altitude of 4,200 meters. Detailed accounts of these experiments are given in References 1, 37, 38 and 39.

These initial investigations using our submillimeter laser heterodyne radiometer system together with an acoustooptic spectrum analyzer have generated further development toward a second generation unit which is more compact and potentially more efficient for a flight oriented package. Design information has been produced to enhance the current AOS I and AOS II devices into a rack-mounted version with a more compact data analysis package.

ACKNOWLEDGEMENTS

The authors wish to acknowledge the work done by Dr. Gerhard Koepf over the course of several years in developing the submillimeter heterodyne radiometer and in using it for spectroscopic measurements with the RF spectrum analyzer and with AOS I. They also wish to acknowledge the pioneering work done by Nelson McAvoy, formerly of the Instrument Electro-Optics Branch, in conceiving and initiating the development of the radiometer.

The authors wish also to express their thanks to David Buhl of the Infrared and Radio Astronomy Branch for providing the RF spectrum analyzer which he developed and for helping to set it up and use it to take spectroscoptic measurements, to Gordon Chin of the Infrared and Radio Astronomy Branch for doing the same thing with the acoustooptic spectrum analyzer which he developed, to Dr. John Hillman of the same branch for several valuable discussions on his theoretical calculations of the absorption line frequencies and strengths for the vibrational ground state of hydrogen peroxide, and to Dr. Nabil Lawandy, formerly of the Instrument Electro-Optics Branch, for very valuable help in understanding molecular spectroscopy over the course of many months.

REFERENCES

1. G. A. Koepf, "Sub Millimeter Laser Heterodyne Radiometry/Spectroscopy," Final Project Report, NASA Contract No. NAS5-26030, Phoenix Corporation, McClean, Virginia, July 1981.

2. R. L. Poynter and H. M. Pickett, "Submillimeter, Millimeter and Microwave Spectral Line Catalogue," NASA/Jet Propulsion Laboratory, JPL Publication 80-23, Revision 1, June 1, 1981.

3. H. R. Fetterman, B. J. Clifton, P. E. Tannenwald, C. D. Parker and H. Penfield, "Submillimeter Heterodyne Detection and Harmonic Mixing Using Schottky Diodes," IEEE Trans. on Microwave Theory Tech., Vol. MIT-22, No. 12, p. 1013, 1974.

4. H. R. Fetterman, "Submillimeter-Wave Optically-Pumped Molecular Lasers," Microwave Journal, Vol. 17, p. 35, 1974.

5. H. R. Fetterman, B. J. Clifton, P. E. Tannenwald and C. D. Parker, "Submillimeter Detection and Mixing Using Schottky Diodes," Applied Physics Letters, Vol. 24, p. 70, 1974.

6. G. A. Koepf, "Submillimeter-Wave Laser Operating in a Passive Q-Switched Intracavity Pump Mode," Applied Physics Letters, Vol. 31, p. 272, Aug. 15, 1977.

7. B. J. Clifton, "Schottky Barrier Diodes for Submillimeter Heterodyne Detection," IEEE Trans. on Microwave Theory and Techniques, MIT-25, No. 6, p. 457, 1977.

8. R. A. Murphy, C. O. Boxler, C. D. Parker, H. R. Fetterman, P. E. Tannewald, B. J. Clifton, J. P. Donnelly and W. T. Lindley, "Submillimeter Heterodyne Detection with Planar GaAs Schottky-Barrier Diodes," IEEE Trans. on Microwave Theory and Techniques, MIT-25, No. 6, p. 494, 1977.

9. N. R. Erickson, "A Directional Filter Diplexer using Optical Techniques for Millimeter to Submillimeter Wavelengths," IEEE Trans. on Microwave Theory and Techniques, Vol. MIT-25, No. 10, p. 865, Oct. 1977.

10. G. A. Koepf and N. McAvoy, "Design Criteria for Optically Pumped FIR Laser Cavities," IEEE Jour. of Quantum Electronics, Vol. QE-13, p. 418, 1977.

11. G. A. Koepf, "CW Operation of an Intracavity Pumped Molecular Submillimeter Wave Laser," IEEE Jour. of Quantum Electronics, Vol. QE-13, p. 732, 1977.

12. H. R. Fetterman, "Advanced Schottky Diode Concepts," Proc. SPIE Symposium, Vol. 105, 1977.

13. G. A. Koepf and K. Smith, "The CW-496 Micrometer Methylfluoride Laser: Review and Theoretical Predictions," IEEE Jour. of Quantum Electronics, Vol. QE-14, p. 333, May 1978.

14. G. A. Koepf, "The Scaling of the CW Optically Pumped Submillimeter Laser," Achiv fur Electrishe Ubertragung, Vol. 32, p. 183, May 1978.

15. H. R. Fetterman, P. E. Tannenwald, B. J. Clifton, C. D. Parker, W. D. Fitzgerald and N. R. Erickson, "Far IR Heterodyne Radiometric Measurements with Quasi-Optical Schottky Diode Mixers," Applied Physics Letters, Vol. 33, p. 151, 1978.

16. H. R. Fetterman, P. E. Tannewald, B. J. Clifton, R. A. Murphy and C. D. Parker, "Advances in Schottky Diode Receivers and Planar GaAs Diode Detectors," Third International Conference on Submillimeter Waves and their Applications, Guilford, England, 1978, Digest.

17. R. A. Murphy, G. D. Alley, C. O. Bonler, H. R. Fetterman, P. E. Tannewald and B. J. Clifton, "Submillimeter Wavelength Surface-Oriented Diode Mixers," International Microwave Symposium Digest, Ottowa, Canada, 1978.

18. H. R. Fetterman, P. E. Tannenwald, B. J. Clifton, C. D. Parker, W. D. Fitzgerald and H. E. Erickson, "High Sensitivity Submillimeter Heterodyne Receiver," International Microwave Symposium Digest, Ottowa, Canada, 1978.

19. R. A. Murphy and B. J. Clifton, "Surface-Oriented Schottky Barrier Diodes for Millimeter and Submillimeter-Wave Applications," International Electron Devices Meeting, Washington, D. C., Digest, p. 124, 1978.

20. F. E. Tannenwald, "Advances in GaAs Schottky Diode Submillimeter Heterodyne Receivers and Radiometers," Proc. of the AGARD/NATO Symposium on Millimeter and Submillimeter Wave Propagation and Circuits, Munich, Germany, 4-8 Sept., 1978.

21. G. A. Koepf, Proc. Heterodyne Systems and Technology Conference, Williamsburg, Va., 1980.

22. G. A. Koepf, H. R. Fetterman and N. McAvoy, Intern. J. Infrared and Millimeter Waves, Sept. 1980.

23. D. Buhl, "Instruction Manual for the 64 Channel Filterbank Spectrometer," Infrared and Radio Astronomy Branch, NASA Goddard Space Flight Center, Greenbelt, Md.

24. D. Casasent, "Optical Signal Processing," Electro-Optical Systems Design, June, 1981, pp. 39-46.

25. A. Korpel, "Acousto-Optics – A Review of Fundamentals," Proc. of the IEEE, Vol. 69, No. 1, Jan. 1981, p. 48.

26. E. H. Young, Jr. and S. Yao, "Design Considerations for Acousto-Optic Devices," Proc. of the IEEE, Vol. 69, No. 1, Jan. 1981, p. 54.

27. W. Rhodes, "Acousto-Optic Signal Processing: Convolution and Correlation," Proc. of the IEEE, Vol. 69, No. 1, Jan. 1981, p. 65.

28. T. Turpin, "Spectrum Analysis Using Optical Processing," Proc. of the IEEE, Vol. 69, No. 1, Jan. 1981, p. 79.

29. G. Chin, D. Buhl and J. Florez, "Acousto-optic Spectrometer for Radio Astronomy," SPIE Vol. 231, International Optical Computing Conference, 1980.

30. Townes and Schawlow, "Microwave Spectroscopy," McGraw-Hill, N.Y., 1955.

31. S. S. Penner, "Quantitative Molecular Spectroscopy and Gas Emissivities," Addison-Wesley, Mass., 1959.

32. Amnon Yariv, "Quantum Electronics," John Wiley & Sons, N.Y., 1967.

33. I. S. Gradshteyn and I. M. Ryzhik, "Table of Integrals, Series and Products," Academic Press, N.Y., 1980.

34. Kraus, "Radio Astronomy," McGraw-Hill, 1966.

35. W. R. Stabnow, "Submillimeter Wave Laser Heterodyne Spectrometer System Software User Manual/Programmer Documentation," GSFC Code 723 In-House Report, April 1982.

36. J. Hillman, Internal Correspondence.

37. G. A. Koepf, D. Buhl, G. Chin, D. D. Peck, H. R. Fetterman, P. E. Tannenwald and B. J. Clifton, "CO (J=5←6) Distribution in Orion and Detection in Other Galactic Sources," Informal report.

38. G. A. Koepf, H. R. Fetterman, P. F. Goldsmith, B. J. Clifton, D. Buhl, N. R. Erickson, D. D. Peck, N. McAvoy and P. E. Tannenwald, "Groundbased Heterodyne Observation of CO at 691 GHz," Fifth International Conference on Millimeter and Infrared Waves, Wurzburg, Germany, Oct. 1980.

39. H. R. Fetterman, G. A. Koepf, P. F. Goldsmith, B. J. Clifton, D. Buhl, N. R. Erickson, D. D. Peck, N. McAvoy and P. E. Tannenwald, "Submillimeter Heterodyne Detection of Interstellar Carbon Monoxide at 434 Micrometers," Science, 6 February 1981, Volume 211, pp. 580-582.

APPENDIX

DERIVATION OF THE RELATION BETWEEN THE OBSERVED DATA AND THE ABSORPTION COEFFICIENT

The spectra shown in this report are actually plots of a quantity Q which is a simple function of the (integrated) voltages at the outputs of the spectrum analyzer channels. What we really want, of course, is a plot showing the value of the absorption coefficient for each channel. We therefore need to find the relationship between the measured quantity Q and the absorption coefficient. To do this it is necessary to follow in detail what happens to the signal as it passes through the radiometer. It is convenient to start by finding the relation between Q and the apparent temperatures seen at the input to the Schottky diode; these will then be related back to the absorption coefficient.

The measured quantity Q is defined by:

$$Q = \frac{(S-R)/R}{(S_0-R)/R} \tag{A1}$$

where S, S_0 and R all represent voltages at the output of any given one of the spectrum analyzer channels; S denotes the output voltage when the gas sample cell is filled with an absorbing gas (S stands for "signal"), S_0 denotes the output voltage when the gas cell is evacuated and R denotes the output voltage when only a reference signal is incident on the whisker antenna of the Schottky diode. We now need to express S, S_0 and R in terms of the apparent temperatures at the input to the Schottky diode; this requires tracing the signal through the radiometer, from the input of the diode to the output of the spectrum analyzer. To do this we first need to understand clearly the double-sideband mixing action of the diode.

The output current of the diode is a highly nonlinear function of the input voltage. For any nonlinear device, the output corresponding to an input which is the sum of two signals consists of products of powers of the two signals, as can be seen by expanding the output as a Taylor series in the input variable. If the simple product of the two signals is dominant in the output (except possibly for a constant term and the signals themselves), the device can be used as a multiplier. If one of the two signals is a sinusoid, the effect of the device is then to merely shift the spectrum of

the other signal both up and down along the frequency axis, by the frequency of the sinusoid. Used in this manner, the device functions as a mixer; i.e., as a downward frequency shifter. The other signal is then available in a lower frequency range, but with its spectrum otherwise unchanged. The situation for our device is indicated in Figure A1.

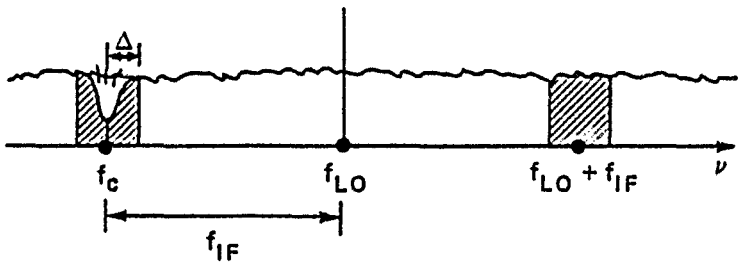

Figure A1. Input Spectrum to the Mixer

In Figure A1 the horizontal axis shows frequency increasing toward the right. The subscripts c, LO and IF denote the absorption line center frequency, the local oscillator frequency and the first IF frequency, respectively. The wavy line indicates the blackbody spectral distribution, from whatever blackbody source is being used, and the dip in the spectrum at the left represents the absorption line being investigated. The local oscillator frequency is shown as being above the absorption line, although it may in some cases be below it. By the Raleigh-Jeans approximation to the blackbody spectral distribution (which is valid for submillimeter wavelengths),

$$B = 2kT/\lambda^2 \qquad (A2)$$

where B is the brightness, k is Boltzmann's constant, T is the absolute temperature of the blackbody source and λ is the wavelength. Because the percentage variation in the wavelength is very small over the frequency band indicated in Figure A1, it is clear that B is nearly constant over the frequency band.

The action of the Schottky diode mixer can be imagined as shifting the entire spectrum shown in Figure A1 down along the frequency axis so that the local oscillator frequency f_{LO} is at zero frequency. If the local oscillator frequency lies above the absorption line, the spectrum of the line can be imagined to reflect off the zero-frequency vertical axis (if we consider the spectrum to be

mathematically represented by only positive frequencies) and to move upward again until the line center comes to rest at the frequency $f_{IF} = f_{LO} - f_c$ (the first intermediate frequency). The absorption line spectrum then overlays a pure noise spectrum (i.e., the blackbody source spectrum) in the band $f_{IF} \pm \Delta$. This situation is depicted in Figure A2. If the local oscillator frequency happens to lie below the absorption line the situation is essentially the same, except that in this case the line spectrum is not transformed into a mirror image of itself. If we assume that the absorption lines we will be dealing with are symmetrical, then we can ignore any mirror inversion of the spectrum.

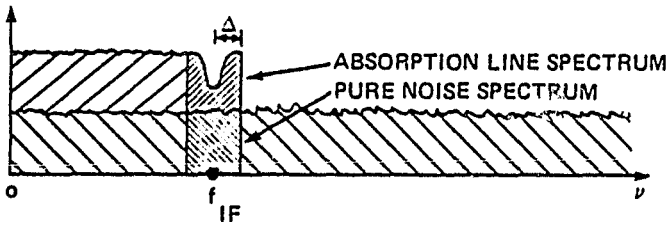

Figure A2. Down-Shifted Spectrum

This intermediate frequency spectrum is then amplified by a low-noise amplifier and passed through a filter which passes only the band $f_{IF} \pm \Delta$ (shown darkly shaded in Figure A2). It is important to note that this band contains two overlapping spectra: the absorption line spectrum plus pure noise. In this sense the action may be described (loosely) as double-sideband detection.

The band $f_{IF} \pm \Delta$ is then down-shifted a second time, but this time it is not altered (except for a scale factor), because the noise outside of the band has been filtered out. The resulting band $f_{IF} \pm \Delta$ is then passed through a spectrum analyzer which performs a discrete multi-channel spectral analysis of the band (and thus of the absorption line within it).

We are now in a position to relate the voltage of the output of the spectrum analyzer to the apparent temperature at the input to the Schottky diode. The voltage at the output of any given channel of the spectrum analyzer comes from two sources: thermal (blackbody) radiation at the

input to the Schottky diode and noise generated within the receiver itself, from the diode on. (Note that the thermal radiation is itself just noise; the spectral line "signal" is just a variation of the amplitude of this thermal noise along the frequency axis.) If we denote the voltage at the output of a spectrum analyzer channel by $v(\epsilon)$, where ϵ is the frequency deviation from the center of the spectral line, we may write:

$$v(\epsilon) = h\, T(\epsilon) \tag{A3}$$

where $T(\epsilon)$ is the apparent temperature at the input to the diode and h is a factor which takes account of all gains and losses through the receiver, from the diode on, including conversion losses in the diode. Because the two "sidebands" (i.e., the band containing the absorption line and its image on the other side of the local oscillator frequency) differ by only a small frequency, we may assume that they are affected to the same degree by conversion losses in the Schottky diode; at all points downstream in the receiver the two sidebands are in the same frequency band, so that they undergo the same losses and gains. We may thus assume that h does not depend on frequency over the band we are working with; note also that h includes dimensioned conversion factors, since v and T have different dimensions. The temperature T is the sum of two fictitious temperatures:

- The temperature of a fictitious blackbody which, if viewed through empty space, would give the brightness actually incident on the Schottky diode; this brightness is related to T by the Raleigh-Jeans Law (Eq. A2).

- The temperature of a fictitious blackbody which, if its radiation were incident (through empty space) on the diode, would give rise to the output voltage observed in the absence of any true input signal (i.e., the voltage caused by internally generated noise). In other words, this component of T is just the receiver noise referred to the input and expressed as an effective blackbody temperature.

We now must write explicit forms for T, for three distinct cases:

i) The gas sample cell is filled, so that an absorption line is present;

ii) The cell is evacuated;

iii) The input to the diode comes from a reference source.

For the first case we may represent the part of T due to the brightness incident on the diode by $T_{OFF\text{-}LINE} + (T_{OFF\text{-}LINE} - \Delta T(\epsilon))$, where $T_{OFF\text{-}LINE}$ denotes the apparent temperature seen by the diode away from the absorption line and $\Delta T(\epsilon)$ denotes the difference in apparent temperature between the off-line level and a point on the line; note that $T_{OFF\text{-}LINE}$ appears twice because of the two overlapping sidebands. As will be described in more detail below, $T_{OFF\text{-}LINE}$ is the actual temperature of the blackbody source, reduced by internal losses in the gas cell walls and associated windows and mirrors; $\Delta T(\epsilon)$ is the temperature difference due to absorption, also reduced by the same internal loss factor. The part of T due to internally generated noise (i.e., the noise temperature of the receiver) may be represented by $2T_N$, since the noise temperature may be assumed to be constant over the frequency band considered; again the factor of two is due to the two sidebands. Thus we may write T for the first case in the form:

$$T = 2T_{OFF\text{-}LINE} + 2T_N - \Delta T(\epsilon) \tag{A4}$$

The second case is the same, except that ΔT is zero:

$$T = 2T_{OFF\text{-}LINE} + 2T_N \tag{A5}$$

For the third case we have:

$$T = 2T_{REF} + 2T_N \tag{A6}$$

where T_{REF} is the actual physical temperature of a reference body placed right before the receiver (actually, before the diplexer). If we put the three expressions for T given by Eq's. A4, A5 and A6 into Eq. A3, denote the resulting v's by S, S_0 and R, respectively and put those into Eq. A1, we get the measured quantity Q in terms of the apparent temperatures seen by the receiver. Before writing out this relation, however, it is necessary to briefly describe the measurement process as it is carried out in the laboratory. A chopper (a fanlike device with two or more blades) is inserted into the beam just before the diplexer. The rotating blades interrupt the beam emerging from the sample cell several times a second, so that the receiver alternately sees the beam from the cell and one of

the chopper blades, which are at room temperature; these blades supply the reference, T_{REF}. Observations are first made with the sample cell filled with the absorbing gas, for a long enough time to average out the random fluctuations and obtain a good spectrum. The sample cell is then evacuated and the process is repeated. If the elapsed time between the two sets of observations is too great, the value of h (in Eq. A3) may have changed due to drifts in the gains and losses through the receiver. (We assumed that h is independent of frequency over the small range we are working with, but it may vary with time.) Because of this possibility we will attach subscripts to n and to T_N; the subscript 1 refers to the first set of observations with gas in the cell and the subscript 2 refers to the second set of observations with the cell evacuated. Thus we may write:

$$S = h_1(2T_{OFF\text{-}LINE} + 2T_{N1} - \Delta T(\epsilon))$$

$$S_0 = h_2(2T_{OFF\text{-}LINE} + 2T_{N2})$$

$$R = h_{1,2}(2T_{REF} + 2T_{N\,1,2})$$

where the subscripts in the expression for R depend on whether R is measured in the first or second set of observations. If we put these expressions into Eq. A1 we obtain the relation between the measured quantity Q and the apparent temperatures seen by the radiometer; before simplification this relation takes the form:

$$Q = \frac{[h_1(2T_{OFF\text{-}LINE} + 2T_{N1} - \Delta T(\epsilon)) - h_1(2T_{REF} + 2T_{N1})]/h_1(2T_{REF} + 2T_{N1})}{[h_2(2T_{OFF\text{-}LINE} + 2T_{N2}) - h_2(2T_{REF} + 2T_{N2})]/h_2(2T_{REF} + 2T_{N2})}$$

From this formula for Q it is apparent why Q was defined the way it was: it is so that all the h's and T_N's cancel, provided (and this is essential) that the elapsed time between the observations with gas in the cell and with the cell evacuated is small enough so that no appreciable drift has occurred in the receiver between the two sets of observations. If this is the case then the quantity Q is independent of the noise temperature of the receiver (and of the gain or loss in any component). The expression for Q then takes the simplified form:

$$Q = 1 - \tfrac{1}{2}\frac{\Delta T(\epsilon)}{(T_{OFF\text{-}LINE} - T_{REF})} \qquad (A7)$$

It is important to note one other property of the definition of Q: the value of Q remains the same under any linear transformation of the output voltage v. Thus if Eq. A3 were to be replaced by a relation of the form $v(\epsilon) = aT(\epsilon) + b$, the same final formula for Q would have resulted. This means that the value of Q does not depend on the zero reference used to define the ouput voltage v, or on any change of scale factor, provided only that v is defined the same way in measuring all three of the quantities S, S_0 and R.

We now must relate the quantities appearing in Eq. A7 to the absorption coefficient of the gas being investigated. To do this we need to apply the theory of radiation transfer to the gas cell with the blackbody source at one end, to calculate the apparent temperature at the other end (just before the diplexer). The theory (too lengthy to give here) yields the following relation:

$$T_{REC}(\epsilon) = T_{BB}\, e^{-(\alpha(\epsilon) + \alpha_{LOSS})\ell} + T_{GAS}(1 - e^{-(\alpha(\epsilon) + \alpha_{LOSS})\ell} \qquad \text{(A8)}$$

where $\alpha(\epsilon)$ is the absorption coefficient, α_{LOSS} is the loss coefficient due to internal losses in the gas cell (wall absorption plus losses in windows, etc.), ℓ is the length of the cell, $T(\epsilon)$ is the apparent temperature at the far end of the cell (just before the receiver), T_{BB} is the physical blackbody temperature and T_{GAS} is the physical temperature of the gas in the cell. The first term on the right-hand side of Eq. A8 is due to absorption by the gas; the second term takes account of emission from the gas, assuming local thermodynamic equilibrium. The temperature of the blackbody source was purposely made quite high, so that the absorption term would be dominant and the emission term could be neglected. However, we will carry the emission term through the calculations, for the sake of clarity. Using Eq. A8 we may immediately write expressions for the off-line apparent temperature and the apparent line depth:

$$T_{OFF\text{-}LINE} = T_{BB}\, e^{-\alpha_{LOSS}\ell} + T_{GAS}(1 - e^{-\alpha_{LOSS}\ell}) \qquad \text{(A9)}$$

and

$$\begin{aligned}\Delta T(\epsilon) &= T_{OFF\text{-}LINE} - T_{REC}(\epsilon) \\ &= e^{-\alpha_{LOSS}\ell}(T_{BB} - T_{GAS})(1 - e^{-\alpha(\epsilon)\ell})\end{aligned} \tag{A10}$$

If we put the two expressions given by Eq's. A9 and A10 into Eq. A7, and if we write $(1-\beta) = e^{-\alpha_{LOSS}\ell}$ (so that β is just the fractional loss of apparent temperature in the gas cell due to internal losses), we obtain:

$$Q(\epsilon) = 1 - \tfrac{1}{2}\frac{1 - e^{-\alpha(\epsilon)\ell}}{1 + \dfrac{T_{GAS} - T_{REF}}{(1-\beta)(T_{BB} - T_{GAS})}} \tag{A11}$$

It is clear that the fraction in the denominator must be small, since T_{REF} is about 300 K (room temperature), T_{BB} is about 1274 K and T_{GAS} is somewhat above room temperature due to heating of the gas ($\beta = 0{,}4$); we may thus write, to a good approximation:

$$Q(\epsilon) \cong \tfrac{1}{2}(1 + e^{-\alpha(\epsilon)\ell}) \tag{A12}$$

Note that we could have arrived at this same approximation by neglecting the second term (the emission term) in Eq. A8. Also it is worth nothing that $\frac{1}{2} < Q \leq 1$, because $0 < \alpha$. If we solve Eq. A12 for the absorption coefficient we obtain the relation we wanted:

$$\alpha(\epsilon) = \frac{1}{\ell} \ln \frac{1}{2Q(\epsilon) - 1} \tag{A13}$$

This gives the absorption coefficient in terms of the measured quantity Q. If the values of the absorption coefficient thus obtained are plotted for each of the spectrum analyzer channels, the result is the absorption line shape, to within the resolution of the analyzer.